CONSTRUCTION MATERIALS CONSULTANTS, INC.

Laboratory Analyses of A Historic Masonry Mortar

Flagstaff Area National Monument
Historic Residence #2
4 Walnut Canyon Road
Flagstaff, Arizona 86004

May 15, 2019
CMC 0419119

TABLE OF CONTENTS

LABORATORY STUDIES OF A MASONRY MORTAR FROM A HISTORIC RESIDENCE IN FLAGSTAFF, ARIZONA

ABSTRACT

As part of the renovation process of the historic Residence #2 constructed between 1938 and 1942 at 4 Walnut Canyon Road in the City of Flagstaff, Arizona, a few masonry mortar fragments were provided to determine the type, composition, and microstructure of the mortar, including the type, grain-size distribution, and mineralogical composition of sand used in the mortar, type(s), chemical, and mineralogical compositions of the binder(s) added, microstructural evidence of any physical and/or chemical deterioration of the mortar from prolonged outdoor exposure, volumetric proportions of binder(s) and sand ingredients in the mix, and finally, suggestions for a suitable mix to match the existing mortar. The mortar was analyzed by comprehensive laboratory examinations, e.g., by following the methods of ASTM C 1324 and RILEM including optical and scanning electron microscopy and X-ray microanalyses (SEM-EDS), chemical analyses (gravimetry), X-ray diffraction (XRD), X-ray fluorescence (XRF), thermal analyses (TGA, DTG, DSC), and ion chromatography.

Based on detailed laboratory studies, the mortar is determined to be representative of a high-lime historic cement-lime mortar similar to many historic lime mortars but containing a subordinate amount of blended cement (made using major amount of Portland cement and minor amount of fly ash) relative to the proportion of lime putty made using **1-part blended cement to 1.1-part dolomitic lime to 8-part sand, which is closely equivalent to a modern day ASTM C 270 Type N cement-lime mortar.**

Optical microscopy has determined the high-lime cement-lime-volcanic/siliceous/calcareous sand composition of the historic mortar from its: (a) characteristic mineralogies of sand and binder, (b) hydrated and carbonated microstructure and composition of paste having an overwhelming porous, ultrafine, severely carbonated lime microstructure with scattered residual Portland cement particles, minor spherical fly ash particles, and associated occasional denser carbonated paste of cement hydration products, and (c) mixed volcanic (basalt, plagioclase feldspar), siliceous (quartz, quartzite, chert, granite, sandstone), and calcareous (limestone) sand, probably derived from the Walnut Canyon. SEM-EDS analyses of paste have confirmed the presence of high-lime dolomitic lime and Portland cement binder components where lime has a magnesian lime composition, which has provided an average paste-cementition index, CI (after Eckel 1922) of 0.89. XRD analysis has confirmed the dominance of quartz from silica sand, subordinate presence of plagioclase feldspar from sand, and abundant calcite from carbonated lime paste and calcareous (limestone) component of sand. XRF studies of acid and alkali-digested filtrates of mortar showed detectable soluble silica from Portland cement component of binder to confirm the lime-cement composition. Predominant endothermic peak from calcite decarbonation in thermal analyses, and high magnesium composition of paste are consistent with use of a dolomitic lime component in the binder, which was probably added as a lime putty where quicklime was manufactured from calcination of a dolomitic limestone. Results obtained from microscopy, chemical analyses, and finally thermal analyses are all consistent, confirmatory to each other, and provided a comprehensive understanding of mortar, which was determined to be prepared from mixing major amount of dolomitic lime putty with subordinate amount of blended (Portland+fly ash) cement, and Walnut Canyon sand.

Based on: (i) the determined high-lime blended cement-dolomitic lime binder composition of mortar from microscopy and chemical analysis; (ii) natural siliceous-calcareous sand compositions of aggregate; and (iii) calculated volumetric proportions of 1-part cement to 1.1-part lime to 8.0-part sand, a possible replacement mortar mix could be made using: (a) Portland or blended cement, and (b) dolomitic hydrated lime (*a la* ASTM C 207) mixed with (c) natural (canyon) sand, having **1-part Portland (or blended) cement to 1 to $1^1/_2$-part dolomitic hydrated lime to $4^1/_2$ to 6-part canyon sand**. Overall appearance of the final mortar would depend on a match on sand that constitutes the dominant proportion of the mortar. Sand to be used should match in color to the color of sand in the present mortar, preferably from the similar source, free of any debris, unsound, clay particles, or any potentially deleterious constituents, should conform to the size requirements of ASTM C 144 for masonry sand, and should be durable. Due to years of atmospheric weathering and alterations, an exact match in color to the existing mortar may not be possible, which, even if possible, could alter in future due to continued atmospheric weathering in the presence of oxygen, moisture, and other elements.

INTRODUCTION

Located at 4 Walnut Canyon Road in the City of Flagstaff, Arizona the historic Residence #2 (Figure 1) was reportedly constructed between 1938 and 1942. The subject building is nearly 100 years old and some mortar joints are beginning to fail, most notably around the chimney.

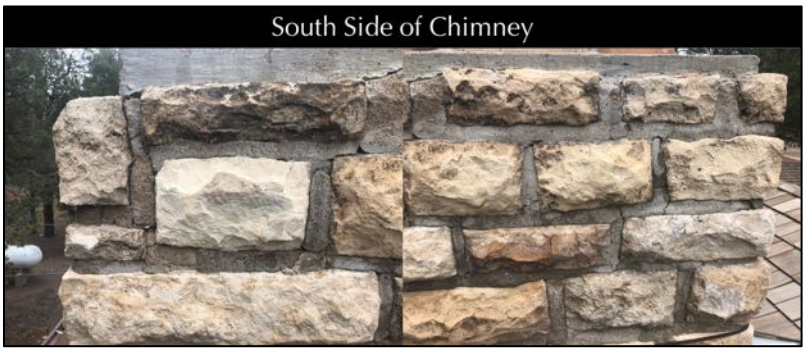

Figure 1: South Side of Chimney of the Historic Residence #2 at Walnut Canyon Road.

As part of the renovation process, a hardened mortar sample from the southside of chimney was provided for detailed laboratory investigations to determine the type, composition, and microstructure of the mortar, including the type, grain-size distribution, and mineralogical composition of sand used in the mortar, type(s), chemical, and mineralogical compositions of the binder(s) added, microstructural evidence of any physical and/or chemical deterioration of the mortar from exposures, volumetric proportions of binder(s) and sand ingredients in the mix, and finally, suggestions for a suitable mix to match with the existing mortar.

Figure 2 shows fragmented pieces of mortar, as received and viewed from different sides, weighing 11.97 grams, and measuring 40 mm × 30 mm × 5 mm in nominal length × width × thickness for the largest piece. Representative fragments were selected for optical and electron microscopy and microanalyses, X-ray diffraction and X-ray fluorescence, chemical analyses (soluble silica content, insoluble residue, loss on ignition, and ion chromatography), sand extraction and sieve analysis, and thermal analyses.

Figure 2: Mortar sample from southside of chimney, as received in multiple fragments.

METHODOLOGIES[1]

Until 1970-1980, characterization of masonry mortars were mostly based on traditional wet chemical analysis (Jedrzejewska, 1960, Stewart and Moore, 1981) where interpretation of results were often difficult if not impossible without a good knowledge of the nature of different ingredients. The majority of later characterization proposed optical microscopy (Erlin and Hime 1987, Middendorf et al. 2000, Elsen 2006) as the first step in identification of different components or mortar based on which other analytical techniques including wet chemistry are performed, e.g., scanning electron microscopy and X-ray microanalysis, X-ray diffraction, X-ray fluorescence, atomic absorption, thermal analysis, infrared spectroscopy, etc. (Bartos et al. 2000, Elsen 2006, Callebaut et al. 2000, Erlin and Hime 1987, Goins 2001, 2004, Groot et al. 2004, Doebley and Spitzer 1996, Chiari et al. 1996, Middendorf et al. 2000, 2004, 2005, Leslie and Hughes 2001, Martinet and Quenee 2000, Valek et al., 2012, Jana 2005, 2006). The choice of

[1] For details on laboratory facilities for testing of masonry mortar, visit www.cmc-concrete.com.

appropriate analytical technique depends mainly on the questions that have to be addressed, and, on the amount of material available.

Purposes of laboratory testing are: (a) to document a historic or modern masonry mortar by examining its sand and binder components, proportions of various ingredients, and their effects on properties and performance of the mortar, (b) evidence of any chemical or physical deterioration of mortar from unsoundness of its ingredients to effects of potentially deleterious agents from the environment (e.g., salts), (c) records of later repointing events and their beneficial or detrimental effects on the performance of the original mortar and masonry units, and finally, (d) an assessment of an appropriate restoration mortar to ensure compatibility with the existing mortar.

Currently there are two standardized procedures available that describe various laboratory techniques for analyses of masonry mortars with special emphases on historic mortars. One is ASTM C 1324 "Standard Test Method for Examination and Analysis of Hardened Masonry Mortar," which includes detailed petrographic examinations, followed by chemical analyses, along with various other analytical methods to test masonry mortars as described in various literatures, e.g., XRD, thermal analysis, and infrared spectroscopy. The second one is the RILEM method described in Middendorf et al. (2004, 2005).

The present mortar was tested by following these established methods of ASTM C 1324, and RILEM, which include detailed petrographic examinations i.e. optical and scanning electron microscopy and X-ray microanalyses (SEM-EDS), followed by chemical analyses (gravimetry, acid digestion), X-ray fluorescence (XRF), X-ray diffraction (XRD), and thermal analyses (TGA, DTG, and DSC). Mortar sample was first photographed with a digital camera, scanned on a flatbed scanner, and examined in a low-power stereomicroscope for the preliminary examinations, e.g., to screen any unusual pieces having different appearances, e.g., representing contaminants from prior pointing episodes. Representative subset pieces of interest are then selected for: (a) optical microscopy and (b) scanning electron microscopy and X-ray microanalysis for chemical and mineralogical compositions, and microstructures of sand, paste, and overall mortar/mortar, (c) acid digestion, preferably from un-pulverized or lightly pulverized sample for sand extraction for grain size distribution, (d) loss on ignition from ambient to 950°C temperatures for free and hydrate water, and carbonate contents, (e) acid digestion for determination of insoluble residue content, (f) cold acid and hot alkali digestions for determination of soluble silica content from hydraulic binder if any, after pulverizing a subset to finer than 0.3 mm size, and, (g) ultra-fine pulverization (<44-micron) of a subset for XRD, XRF, and thermal analysis. Any additional analyses, if needed, e.g., water digestion of mortar for determination of water-soluble salts by ion chromatography, or, Fourier-transform infrared spectroscopy of mortar for determining any organics added, etc. are done on as-needed basis from the remaining set.

Information obtained from petrographic examinations is crucial to devise appropriate guidelines for chemical methods, and, to properly interpret the results of chemical analyses. For example, detection of siliceous versus calcareous versus argillaceous components of aggregates in sample, or, the presence of any pozzolan in the binder (slag, fly ash, ceramic dusts, etc.) from petrography restricts which chemical method to follow, and how to interpret the results of such analyses, e.g., acid-insoluble residue contents. Therefore, a direct chemical analysis e.g., acid digestion of a mortar without doing a prior petrographic examination to determine the types of aggregates and binder used could lead to highly erroneous results and interpretation. Armed with petrographic and chemical data, and based on assumed compositions and bulk densities of the sand and the binder(s) similar to the ones detected from petrographic examinations, volumetric proportions of sand and various binders present in the examined sample can be calculated. The estimated mix proportions from such calculations can provide a rough guideline to use as a starting mix for mock-up mix during formulation of a pointing mortar to match with the existing mortar.

Optical Microscopy

The main purposes of optical microscopy of masonry mortar are characterization of: (a) aggregates, e.g., type(s), chemical and mineralogical compositions, nominal maximum size, shape, angularity, grain-size distribution, soundness, alkali-aggregate reactivity, etc. (b) paste, e.g., compositions and microstructures to diagnose various type(s) of binder(s) used, (c) air, e.g., presence or absence of air entrainment, air content, etc., (d) alterations, e.g., lime leaching, carbonation, staining, etc. due to interactions with the environmental agents during service, and effects of such alterations on properties and performance of mortar; and (e) deteriorations, e.g., chemical and/or

physical deteriorations during service, cracking from various mechanisms, salt attacks, possible reasons for the lack of bond if reported from the masonry unit, etc. Fragments selected from preliminary examinations for microscopy are sectioned, polished, and thin-sectioned (down to 25-30 micron thickness) preferably after encapsulating and impregnating with a dyed-epoxy (Fig. 3) to improve the overall integrity of the sample during precision sectioning and grinding, and to highlight porous areas, voids, and cracks. Prepared sections are then examined in a high-power (up to 100X) Stereozoom microscope having reflected and transmitted-light, and plane and crossed polarized-light facilities, and eventually in a high-power (up to 600X) petrographic microscope equipped with transmitted, reflected, polarized, and fluorescent-light facilities. Capturing high-resolution photomicrographs from these microscopes via digital microscope cameras with image analyses software are an integral part of documentations during petrographic examinations.

Therefore, four essential steps followed during optical microscopy are: (a) visual examination of as-received, fresh fractured, and sectioned surfaces of mortar in a stereo-microscope, (b) preparation of a large-area (50 × 75 mm) thin section of homogeneous thickness (25-30 micron), (c) observation of thin section in a transmitted-light stereo-zoom microscope from 5X to 100X preferably with polarized-light facilities to observe large-scale distribution of sand and mortar microstructure, and finally (d) observation of thin section in a polarized-light (petrographic) microscope from 40X to 600X equipped with transmitted and reflected polarized and fluorescent-light facilities for examinations of sand and binder compositions and microstructures.

For thin section preparation, representative fragments are oven-dried at 40°C to a constant mass and placed in a flexible (e.g., molded silicone) sample holder, then encapsulated with a colored dye-mixed (e.g., blue dye commonly used in sedimentary petrography, or, fluorescent dye, Elsen 2006) low-viscosity epoxy resin under vacuum to impregnate the capillary pore spaces of mortar, improve the overall integrity of sample during sectioning by the cured epoxy, highlight porous areas of mortar, alterations, cracks, voids, reaction products, etc. The epoxy-encapsulated cured solid block of sample is then de-molded, sectioned if needed, and processed through a series of coarse to fine grinding on metal and resin-bonded diamond grinding discs with water or a lubricant, eventually a perfectly flat clean ground surface is glued to a frosted large-area (50 × 75 mm) glass slide. Careful precision sectioning and precision grinding of the sample is then done in a thin-sectioning machine till the thickness is down to 50 to 60 micron. Final thinning down to 25 to 30 micron thickness is done on a glass plate with fine (5-15 micron) alumina abrasive. Thin section is eventually polished with various fine (1 micron to 0.25 micron size) diamond abrasives on polishing wheels suitable for examinations in a petrographic microscope, and eventually in SEM-EDS. Sample preparation steps are described in Jana (2006).

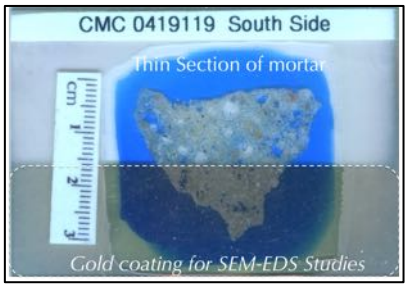

Figure 3: Blue dye-mixed epoxy-impregnated large-area (50 × 75 mm size) thin section prepared for optical microscopy. The bottom half of thin section was coated with a conductive gold film for SEM-EDS analyses.

More elaborate steps followed during optical microscopy include: (a) visual examinations of sample as-received to select fragments for detailed optical microscopy; initial digital and flatbed scanner photography of sample as-received; (b) low-power stereomicroscopic examinations of saw-cut and freshly fractured sections of sample for evaluation of variations in color, grain-size and appearances of sand, and the nature of the paste; (c) examinations of oil immersion mounts for special features and materials in a petrographic microscope; (d) examinations of colored (blue or fluorescent) dye-mixed epoxy-impregnated polished thin sections in a transmitted-light Stereozoom microscope for determination of size, shape, angularity, and distribution of sand, as well as abundance and distribution of void and pore spaces that are highlighted by the colored dye-mixed epoxy; (e) image analyses of photomicrographs of thin sections for estimations of pores, voids, intergranular open spaces, and shrinkage microcracks by using Image J or other image analysis software where multiple photomicrographs are collected in plane polarized light mode by using a high-resolution Stereozoom microscope equipped with transmitted and polarizing light facilities and stitched to get an adequate representative coverage; (f) examinations of colored (blue or fluorescent) dye-mixed epoxy-impregnated polished thin sections in a petrographic

microscope for detailed compositional, mineralogical, textural, and microstructural analyses of aggregates and binders, along with diagnoses of evidence of any deleterious processes and alterations (e.g., lime leaching, precipitation of secondary deposits and alteration products, salts); (g) examinations of polished thin or solid section in reflected-light (epi-illumination) mode of petrographic microscope after etching the surface with acids to identify various non-hydrated hydraulic phases (e.g., C_2S, C_3S, C_3A, etc., Middendorf et al., 2005); (h) examinations of any physical or chemical deterioration or signs of improper construction practices from microstructural evidences; (i) stereo-microscopical examinations of size, shape, and color variations of sand extracted after hydrochloric acid digestion; and finally (j) selection of areas of interest to be examined by scanning electron microscopy.

Scanning Electron Microscopy & Microanalysis by Energy-Dispersive X-ray Spectroscopy (SEM-EDS)

Methods followed in SEM-EDS include: (a) secondary electron imaging (SEI) to determine the microstructure and morphology of the examined surface of sample, (b) backscatter electron (BSE) imaging to determine compositions of various phases from various shades of darkness/grayness/brightness from average atomic numbers of phases from the darkest pore spaces to brightest iron minerals (e.g., thaumasite, periclase, ettringite, quartz, dolomite, monosulfate, gypsum, calcite, C-S-H, aluminate, calcium hydroxide, belite, alite, free lime, and ferrite having progressively increasing average atomic numbers and brightness in BSE image), (c) X-ray elemental mapping (dot mapping) of an area of interest to differentiate various phases, (d) point-mode or area (raster)-mode analysis of specific area/phase of interest on a polished thin or solid section, and (e) average compositional analysis of a specific phase or an area on a polished thin or solid section or small subset of a sample.

The main purposes of SEM-EDS studies are to: (a) observe the morphologies and microstructures of various phases of sand and binder, (b) characterize the typical fine-grained microstructure of hydrated, carbonated, and hydraulic components of binder that are too fine to be examined by optical microscopy and are not well crystallized to be detected by XRD; (c) determine major element oxide compositions, and compositional variations of paste, and from that determine the type of binder(s) used, especially to differentiate non-hydraulic calcitic and dolomitic lime mortars from hydraulic lime varieties (e.g., from silica contents of paste), natural cements (e.g., from silica and magnesia contents), pozzolans, slag cements, Portland cements, etc. all from their characteristic differences in compositions and hydraulicities (e.g., cementation index of Eckel 1922); (d) determine composition of residual hydraulic phases to assess the raw feed and calcination processes used in manufacturing of binder; (e) assess hydration, carbonation, and alteration products of binders, (f) investigate effects of various alterations of paste during service and its role on properties and performance of mortar, (g) detect salts and other potentially deleterious constituents, (h) detect pigments and fillers, (i) examine compositional variations across multiple mortars installed, etc.; and eventually (j) complement and confirm the results of optical microscopy.

Due to characteristic difference in compositions of pastes made using various binders, e.g., non-hydraulic lime (CaO dominates over all other oxides), variably hydraulic lime (CaO with variable SiO_2 contents depending on degree of hydraulicity), dolomitic lime (high CaO and MgO), natural cement (CaO, SiO_2, Al_2O_3, and MgO contents are high, high MgO and FeO contents are characteristic), and Portland cement (CaO and SiO_2 contents are higher than all other oxides), SEM-EDS analysis of paste is a powerful method for detection of the original binder components in the sample. Effects of chemical alterations and various chemical deteriorations of a mortar (e.g., lime leaching, secondary calcite precipitates, gypsum deposits, etc.) can also be detected by SEM-EDS.

SEM-EDS analysis was done in a CamScan Series 2 scanning electron microscope equipped with a high-resolution column 40Å tungsten, 40 kV electron optics zoom condenser 75° focusing lens operating at 20 kV, equipped with a variable geometry secondary electron detector, backscatter electron detector, EDS detector for observations of microstructures at high-resolution, compositional analysis, and quantitative determinations of major element oxides from various areas of interest, respectively. Revolution 4Pi software was used for digital storage of secondary electron and backscatter electron images, elemental mapping, and compositional analysis along a line, or on a point or an area of interest. Portion(s) of interest on the polished 50 mm × 75 mm size thin section used for optical microscopy were subsequently coated with carbon or gold-palladium film and placed on a custom-made aluminum sample holder to fit inside the large multiported chamber of CamScan SEM equipped with the

eucentric 50 × 100 mm motorized stage. Usually, features of interest from optical microscopy are marked on the thin section with a fine-tipped conductive marker pen for further observations in SEM. Alternately, solid polished section or grain mount from phases or areas of interest can also be examined. Procedures for SEM examinations are described in ASTM C 1723 and Sarkar et al. (2000).

Acid Digestion

Acid digestion is perhaps the most commonly used test of masonry mortar, which is done to: (a) extract sand from sample by dissolving out the binder fractions so that grain-size distribution of sand can be done by sieve analysis, and (b) assess insoluble sand content in the sample. Sand content after acid digestion is determined both from: (a) 1.00 gram of pulverized sample (finer than 0.3 mm size) digested in 50-ml dilute (1+3) HCl (heated rapidly but below boiling), and, (b) from digesting a representative bulk sample *per se* (for harder mortars or mortars perhaps with light pulverization) in multiple fresh batches of (1+3) HCl at ambient temperature. The former usually gives better result due to small amount, pulverization to easily remove the binder fraction for digestion, and use of rapidly heated acid, whereas latter method requires multiple episodes of digestion in fresh acid and is time-consuming. Acid digestion is also done as the first step to determine soluble silica content in a sample as described below, which is contributed from the hydraulic components in binder.

All these goals of acid digestion depend on the assumptions that: (i) sand is siliceous in composition and does not contain any acid-soluble constituents (e.g., carbonates), and, (ii) binder entirely dissolves in acid and does not contain any acid-insoluble constituents (gypsum, clay, etc.). Applicability of acid digestion to assess these tasks should therefore be first verified by optical microscopy to confirm the siliceous nature of sand without any appreciable acid-soluble constituents, and calcareous nature of binder, and none without any appreciable argillaceous (clay) constituents.

For grain-size distribution of sand (for sample found from optical microscopy to contain siliceous sand), a few representative fragments of (preferably not pulverized or lightly pulverized in a porcelain mortar and pestle for harder mortars to break down to smaller size fraction without crushing the sand to retain the original sand size) are selected for digestion in multiple fresh batches of (1+3) dilute hydrochloric acid to dissolve away all binder fractions and extract, wash, and oven-dry the acid-insoluble component of aggregate. Usually multiple episodes of acid digestion in fresh batches of acid and filtration of residues are needed to entirely remove the binder fractions without losing the finer fractions of sand. Sand particles thus extracted are washed, oven-dried, and sieved in an automatic mini sieve shaker through various U.S. Sieves from No. 4 (4.75 mm) through 8 (2.36 mm), 16 (1.18 mm), 30 (0.6 mm), 50 (0.3 mm), 100 (0.15 mm), and 200 (0.075 mm) for determination of the size, shape, angularity, and color of sands retained on various sieves. Grain-size distribution of sand is then compared with ASTM C 144 specifications for masonry sand. Photomicrographs of sand retained on each sieve are then taken with a stereomicroscope to record the sand size, shape, and color variations. For low amount of sample, or, for sample having calcareous sand, image analysis (e.g., ImageJ) on stitched photomicrographs of thin sections taken from multiple areas can be done to determine the sand-size distribution (Elsen et al. 2011).

Cold Acid & Hot Alkali Digestion

Digestion of a pulverized sample of mortar in a cold acid followed by further digestion of residue in a hot alkali hydroxide solution are done to determine the soluble silica content contributed from the hydraulic component of binder, where cold acid digestion usually dissolves most of the binder without affecting the sand, followed by hot alkali hydroxide digestion to dissolve remaining soluble silica from calcium silicate hydrate component of paste or in mortars containing hydraulic binders. The soluble silica content corresponds to the silica mostly contributed from the hydraulic binder components (and a minor amount from any soluble silica component in the aggregates).

For determination of soluble silica content (modified from ASTM C 1324), 5.00 grams of pulverized sample (finer than 0.3 mm size, without excessive fines) is first digested in 100-mL cold (at 3 to 5°C) HCl and filtered through two 2.5-micron filter papers (filtrate#1). The residue with filter papers is then digested again in hot (below boiling)

75-ml NaOH, and filtered through two 2.5-micron filter papers (filtrate# 2). The two filtrates from acid and alkali digestions are then combined, re-filtered twice with 2.5-micron and then through 0.45-micron filter paper to remove any suspended silica fines, brought to 250 ml volume with distilled water, and then used for soluble silica determination by an analytical method, such as atomic absorption spectroscopy (AAS), inductive coupled plasma optical emission spectroscopy (ICP-OES), or X-ray fluorescence spectroscopy (XRF). Multiple steps of filtrations from 2.5-micron to submicron filter papers are necessary to remove any suspended silica from sand that can skew the result. Instrument to be used for such determination must be calibrated with several silica standards in matrices similar to the one used in mortar analysis. An XRF unit calibrated with filtrates from acid-and-alkali-digested series of laboratory-prepared standards of Portland cement and silica sand mortars (moist cured at *w/c* of 0.50 for 30 days) having various proportions of Portland cements (SiO_2 contents of standards ranging from 1 to 10%) were used for determining SiO_2 Kα X-ray intensities from known stoichiometric silica (cement) contents of standards (using exact 5.00 grams as samples) prepared by the same procedure of cold HCl-digestion/filtration/hot NaOH-digestion/2nd filtration/combination of two filtrates/re-filtration steps as followed for mortars or mortars.

One of the standards used for calibration of XRF was re-used as an internal standard as the first sample during analyses of unknown sample. The standard Portland cement-silica sand mortar contained silica sand (finer than 0.3 mmm size) and 20 percent Portland cement (having 20.2% SiO_2). This standard mortar has a stoichiometric 4.04% soluble SiO_2 (i.e. equivalent to 0.202 gram or 202 mg SiO_2 in 250 ml filtrate of 5.00 grams of standard) to verify the accuracy of XRF results.

Soluble silica (SiO_2) content of sample in weight percent = A/B, where A = [*correction factor for standard*, which is 202 / (mg-SiO_2 of standard in 250 ml filtrate from XRF)] × [*ppm-SiO_2 of sample*, which is 4 (for 250 ml to 1L for ppm) × (mg-SiO_2 of sample in 250 ml filtrate from XRF)] × [*filtrate volume in ml used without dilution*, which is 250]; and B = [*Sample weight in grams*, which is 5.00] × [*ppm to wt.% conversion*, which is 10,000]. Recovery of soluble silica in standard after cold-HCl/hot-NaOH digestion is usually 180 to 200 mg. in 250 ml filtrate in XRF (i.e. correction factor of 1.0 to 1.2).

Hydraulic binder content is then calculated as: [(soluble SiO_2, weight percent in sample as calculated above) divided by assumed soluble SiO_2 content in binder] ×100, where assumed SiO_2 contents of binders varies with binder types, e.g., 21% in Portland cement, 20% in natural cement, 27% in slag cement, 7 to 10% in hydraulic lime, etc., or, more preferably, from the average paste-SiO_2 content determined from SEM-EDS.

Weight Losses on Ignition

Losses in weight of a mortar on step-wise heating from ambient to 110°C, 550°C, and 950°C temperatures liberate free water from capillary pore spaces by 110°C, combined water from dehydroxylation of various hydrous phases (calcium silicate hydrate, calcium hydroxide, etc.) by 550°C, and liberation of carbon dioxide from decomposition of carbonated paste and carbonate minerals by 950°C. Such losses in weight are measured by following the procedures of ASTM C 1324 by heating 1.00 gram of pulverized mortar (finer than 0.3 mm) in an alumina crucible in a muffle furnace in a controlled step-wise heating at a heating rate of 10ºC/min. Mortars having hydraulic binders and hydration products of such provide measurable combined water contents after calcination to 550°C, whereas those having high calcareous components (high-calcium lime mortar or mortar having calcareous sand) produce higher weight losses during ignition to 950°C. Usually, a good correlation is found between weight losses at 550°C from dehydration of combined water, and, soluble silica contents contributed from hydraulic binders amongst series of mortars containing variable amounts of hydraulic phases.

X-ray Diffraction (XRD)

X-ray diffraction (XRD) is useful for: (a) determination of bulk mineralogical composition of mortar, including its aggregate and binder mineralogies (e.g., quartz in sand from major diffraction peaks at 26.65º, 20.85º, 50.14º 2θ, or calcite in sand or carbonated lime binder from major peaks at 29.41º, 39.40º, 43.15º 2θ, or Portlandite in

binder from major peaks at 34.09º, 18.09º, 47.12º 2θ); (b) individual primary mineralogies and alteration products of aggregates at various size fractions, and binder phases; (c) detection of dolomitic lime binder from brucite in the sample from major peaks at 38.02º, 18.59º, 50.86º 2θ; (d) detection of use of lime (portlandite), gypsum (11.59º, 20.72º, 29.11º 2θ), or cement binders from their characteristic mineralogies; (e) detection of any potentially deleterious constituents, e.g., deleterious salts, or efflorescence deposits; (f) detection of a mineral oxide-based pigment in sample; and (g) detection of components difficult to detect by microscopical methods.

X-ray diffraction can be done on: (i) pulverized (to finer than 45 micron) portion of bulk sample, or (ii) on the sand extracted from mortar by acid digestion, if sand has a complex mineralogy, or also (iii) on the binder-fraction by separating sand from the binder from a carefully ground sample (in a mortar and pestle) and passing the ground mass through US 200 sieve (75 micron) to collect the fraction rich in binder. XRD pattern of a sample containing silica sand typically shows quartz as the dominant phase that surpasses peaks for all other phases (e.g., calcite, dolomite, clay, secondary deposits); hence binder separation is sometimes useful to detect minor minerals of interest (e.g., salts or pigments). For mortars containing marine shell fragments as sand, aragonite appears with calcite as two calcium carbonate phases from the shell fragments and paste. For binder mineralogy, sample is first dried at 40°C to a constant mass, then carefully crushed without pulverizing the sand, and sieved through a 75-micron opening screen to retain sand-rich fraction on the sieve and obtain the passed binder-rich fraction for further pulverization down to finer than 45 micron. Salts and other soft components can be analyzed from binder fraction. Efflorescence salts on masonry walls are also analyzed routinely in XRD.

For sample preparation, a Rocklab (Sepor Mini-Thor Ring) pulverizer is used to grind sample down to finer than 100 microns. Usually, a few drops of anhydrous alcohol are added to reduce decomposition of hydrous phases from the heat generated from grinding. Approximately 10 grams of sample is ground first in the pulverizer, from which about 8.0 grams of sample is selected, mixed with an appropriate binder (e.g., three Herzog grinding aid pellets from Oxford Instruments having a total binder weight of 0.6 gram for 8 grams of sample for a fixed binder proportion of 7.5 percent); the mixture is then further ground in Rocklab pulverizer and in a McCrone micronizing mill with anhydrous alcohol down to finer than 44 micron size. Approximately 7.0 grams of binder-mixed pulverized sample thus prepared is weighed into an aluminum sample cup and inserted in a stainless steel die press to prepare the sample pellet. A 25-ton Spex X-press is used to prepare 32 mm diameter pellet from the pulverized sample. The pressed pellet is then placed in a custom-made circular sample holder for XRD and excited with the copper radiation of 1.54 angstroms. Sample holders made with quartz or silicon are best for working with very small quantities of sample because these holders create no diffraction peaks between 2° and 90° 2θ (Middendorf et al. 2005).

XRD is carried out in a Siemens D5000 Powder diffractometer (θ-2θ goniometer) employing a long line focus Cu X-ray tube, divergent and anti-scatter slits fixed at 1 mm, a receiving slit (0.6 mm), diffracted and incident beam Soller slits (0.04 rad), a curved graphite diffracted beam monochromator, and a sealed proportional counter. Siemens D 5000 is equipped with (a) a horizontal stage (fixed), (b) an X-ray generator with CuKα, fine focus sealed tube source, (c) large diameter goniometer (600 mm), low divergence collimator, and Soller slits, (d) fixed detector slits 0.05, 0.2, 0.6, 1.0, 2.0, and 6.0, and (e) Scintillation detector. Generator settings used are 40 kV and 30 mA. Tests are usually run at 2θ from 4° to 64° with a step scan of 0.02° and a dwell time of one second. The resulting diffraction patterns are collected by DataScan 4 software of Materials Data, Inc. (MDI), analyzed by Jade software of MDI with ICDD PDF-4 (Minerals 2017) diffraction data. Phase identification, and quantitative analyses were carried out with MDI's Search/Match, Easy Quant, and Rietveld modules, respectively.

X-ray Fluorescence (XRF)

X-ray fluorescence (XRF) is used for determining: (a) major element oxide composition of sample, and, (b) soluble silica content of filtrate after digestion of sample in cold-HCl and hot-NaOH. Major element oxide compositions provide clues about the siliceous sand content of mortar from silica content, type of binder used (e.g., a dolomitic lime or natural cement based binder gives a characteristically higher magnesia than a calcitic lime or Portland cement based binder), calculation of lime content in a cement-lime mortar from bulk CaO content from XRF,

effect of alterations and deteriorations (e.g., salt ingress in a mortar from marine environment can be diagnosed from excessive sodium, sulfate, and chlorine, etc.), etc. A series of standards from Portland cements, lime, gypsum, to various rocks, and masonry cements of certified compositions (e.g., from USGS, GSA, NIST, CCRL, Brammer, or measured by ICP) are used to calibrate the instrument for various oxides, and empirical calculations are done from such calibrations to determine oxide compositions of mortars. For mortars with highly unusual compositions (e.g. severely salt-contaminated or a gypsum-based mortar) a standard-less FP calculation is done to determine the best possible composition.

An energy-dispersive bench-top X-ray fluorescence unit from Rigaku Americas Corporation (NEX-CG) was used. Rigaku NEX-CG delivers rapid qualitative and quantitative determination of major and minor atomic elements in a wide variety of sample types with minimal standards. Unlike conventional EDXRF analyzers, the NEX-CG was engineered with a unique close-coupled Cartesian Geometry (CG) optical kernel that dramatically increases signal-to-noise. By using monochromatic secondary target excitation, instead of conventional direct excitation, sensitivity is further improved. The resulting dramatic reduction in background noise, and simultaneous increase in element peaks result in a spectrometer capable of routine trace element analysis even in difficult sample types. The instrument is calibrated by using various certified (CCRL, NIST, GSA, and Brammer) reference standards of cements and rocks. The same pressed pellet used for XRD for mineralogical compositions is used for XRF to determine the chemical composition.

Thermal Analyses (TGA, DTG, and DSC)

Thermal analyses encompass: (1) thermogravimetric analysis (TGA), which measures the weight loss in a sample as it is heated, where weight loss can be related to specific physical decomposition of a phase of interest at a specific temperature that is characteristic of the phase from which both the phase composition and the abundance can be determined; (2) differential thermal analysis (DTA, or first derivative of TGA i.e. DTG) measuring temperature difference between the sample and an inert standard (Al_2O_3) both are heated at the same rate and time where endothermic peaks are recorded when the standard continues to increase in temperature during heating but the sample does not due to decompositions (e.g., dehydration of hydrous or decarbonation of carbonate phases); the endothermic or exothermic transitions are characteristic of particular phase, which can be identified and quantified using DTA (or DTG); and (3) differential scanning calorimetry (DSC), which follows the same basic principle as DTA, whereas temperature differences are measured in DTA, during heating using DSC energy is added to maintain the sample and the reference material (Al_2O_3) at the same temperature; this energy use is recorded and used as a measure of the calorific value of the thermal transitions that the sample experiences; this is useful for detection of quartz that undergoes polymorphic (α to β form) transitions and no weight loss.

Thermal analyses are done to determine the presence and quantitative amounts of: (a) hydrates (e.g., combined water liberated from paste dehydration during decomposition of calcium-silicate-hydrate component in paste at 180-190ºC); (b) sulfates (gypsum from decompositions at 125ºC, and 185-200ºC, ettringite at 120-130ºC, thaumasite at 150ºC); (c) brucite from its dehydroxylation at 300-400ºC to confirm the presence of dolomitic lime; (d) hydrate water from decomposition of Portlandite component of paste at 400-600ºC; (e) quartz from polymorphic transformation (α to β form) at 573ºC; (f) cryptocrystalline calcite in the carbonated lime matrix from decomposition at 620-690ºC, or magnesite at 450-520ºC, or (g) coarsely crystalline calcite e.g., in limestone by decomposition at 680-800ºC or (h) dolomite at 740-800ºC and 925ºC, and (i) phase transition of belite (C_2S) at 693ºC, etc. Phases are determined from their characteristic decomposition temperatures occurring mostly as endothermic peaks or polymorphic transition temperatures as for quartz.

Simultaneous TGA and DSC analyses were done in a Mettler Toledo TGA/DSC 1 unit on 30-70 mg of finely ground (<0.6 mm) sample in alumina crucible (70 µl, no lid) from 30°C to 1000°C at a heating rate of 10°C/min with high purity nitrogen as purge gas at a flow rate of 75.0 ml/min. TGA/DSC 1 simultaneously measures heat flow in addition to weight change. The instrument offers high resolution (ultra-microgram resolution over the whole measurement range), efficient automation (with a reliable sample robot for high sample throughput), wide measurement range (measure small and large sample masses and volumes) broad temperature scale (analyze samples from ambient to 1100°C), superior ultra-micro balance, simultaneous DSC heat flow measurement (for

simultaneous detection of thermal events, e.g., polymorphic alpha-to-beta transition of quartz and quartz content), and a gastight cell (ensures a properly defined measurement environment).

Fourier Transform Infra-red Spectroscopy (FT-IR)

Fourier-transform infrared spectroscopy (FT-IR) measures interaction between applied infrared radiation and the molecules in the compounds of interest (Middendorf et al. 2005). FT-IR is particularly useful for detection of admixture, additives, and polymer resins, mainly to identify various organic components (functional groups) in mortar (e.g., methyl CH_3, organic acids CO-OH, carbonates CO_3) from their characteristic spectral fingerprints in FT-IR spectrum. FT-IR can also be used for detection of main mineral phases in a hydraulic binder, CSH, carbonates, gypsum, and clays (Middendorf et al. 2005). Organic compounds such as synthetic (e.g., acrylics, polyesters) and natural resins, carbohydrates, colorants, oils and fats, proteins, waxes as well as inorganic compounds, e.g., corrosion products, minerals, pigments, paints, fillers, stone, glass, and ceramics can be detected by this technique.

FT-IR measurements are done in a Perkin Elmer Spectrum 100 FT-IR spectrophotometer running with Spectrum 10 software. Sample is measured using attenuated total reflection (ATR) on a single bounce diamond/ZnSe ATR crystal between a frequency range of 4000 to 650 cm^{-1}. Each run is collected at 4 cm^{-1} resolution with Strong Beer-Norton apodization. Data are collected with a temperature-stabilized deuterated triglycine sulfate (DTGS) detector by placing the sample in contact with the ATR crystal and by applying force from the pressure applicator supplied with the ATR accessory. The application of pressure enable the sample to be in intimate contact with the ATR crystal, ensuring achievement of a high-quality spectrum. Additionally, more conventional KBr pellet is also sometimes used for samples on as-needed basis.

Ion Chromatography

Salts can cause various deteriorations from: (a) mere aesthetic issues of surface efflorescence by precipitation from evaporation of leachates on the surfaces followed by atmospheric carbonation of the precipitates where salts deposit as individual crystals or as crust to (b) more serious internal distress in mortar from crystallization inside the pores (sub-fluorescence or crypto-fluorescence) from expansive forces associated with crystallization of salt from supersaturated solutions. Some common salts are calcium carbonates (e.g., calcite, vaterite), magnesium carbonate (magnesite), sodium carbonate hydrate and bicarbonate (thermonatrite, trona, nahcolite), sulphates (gypsum, thenardite, epsomite, melanterite, mirabilite, glauberite, or ettringite and thaumasite from oxidation of sulfides or cement hydrates), and chlorides (halite, sylvite, calcium oxychloride from deicing salts, salt-bearing aggregates, ground water). X-ray diffraction and SEM-EDS can determine many of these salts as long as they are present in detectable amounts. Ion chromatography is an established technique used for analyses of various water-soluble anions and cations in salts (e.g., chloride, sulfate, and nitrate anions, and magnesium, calcium, alkali, ammonium cations) to assess magnitude of environmental impacts on masonry units and mortars, and subsequent effects of such salt ingress. Samples are pulverized, digested in deionized water to remove all water-soluble salts, then solid residues are filtered out and the water-digested filtrates are analyzed by an ion chromatograph.

Ion chromatography methods are described in ASTM D 4327 "Standard Test Method for Anions in Water by Chemically Suppressed Ion Chromatography." Briefly, an aliquot of 1 gram of pulverized sample (passing No. 50 sieve) was digested in 50 ml distilled water for 6 to 8 hours on a magnetic stirrer at a temperature below boiling point of water; then the digested sample was filtered through two 2.5-micron filter papers using vacuum, followed by a second filtration through micro-filter (0.45 micron) paper, then the filtrate was either used directly or diluted to 100 to 250 ml with distilled water depending on the concentration of anions, and used for analysis to get ppm-level fluoride, chloride, nitrite, bromide, nitrate, phosphate, and sulfate in the water-digested sample in Metrohm 861 Advanced Compact IC. The instrument was calibrated against six different custom-made Metrohm anion standard solutions having all these anions from 0.1-ppm to 100-ppm levels. To check the accuracy of the instrument, a 50-ppm standard solution was run first prior to the analyses of samples.

Laboratory Analyses of Masonry Mortars

Initial Mortar (50 to 100 grams) [Photographed with digital camera & flat-bed scanner, As-received condition, total weight, and dimensions of largest piece are documented]

Intact Pieces (20+ g)

1. Optical Microscopy

I. Perform visual examination of mortar as received, then saw-cut and fractured surfaces and with a low-power stereomicroscope,
II. Take digital and flat bed scanner photos of intact piece(s),
III. Encapsulate the piece for thin section microscopy in a flexible mold with a low-viscosity colored or fluorescent dye-mixed epoxy to highlight voids, pores, cracks, etc.,
IV. Prepare thin section (< 30 micron thickness) and polish the thin section for optical and SEM-EDS analyses,
V. Scan the thin section on a flat-bed scanner with the thin section residue,
VI. Take transmitted light high-power stereo-zoom photomicrographs of thin sections from different areas to be stitched to determine volumes and size distributions of pore spaces and sand grains by Image J,
VII. Take plane and crossed polarized-light photomicrographs of sand and binder fractions in thin section from a petrographic microscope and determine areas for further studies by SEM-EDS,
VIII. Do detailed petrographic examinations to determine the sand and binder compositions, sand mineralogy and texture, binder phases, residual binders, alterations, and products of any deleterious reactions, immersion mounts of specific areas of interest, etc.

2. SEM-EDS

I. Put conductive coating only on the portion of polished thin section intended for SEM-EDS studies from optical microscopy,
II. Take backscatter and/or secondary electron images, and if needed X-ray elemental maps,
III. Select multiple areas on paste to determine oxide compositions and Eckel's cementation indices,
IV. Tabulate the paste composition variations across the backscatter/secondary electron image.
V. Determine chemical compositions of resides left from the original components of the binders, as well as the hydration and carbonation and other alteration products

Lightly hand-ground in a Mortar & Pestle (30+ g)

3. Acid Digestion - Sand Color & Sand Size Distribution (10 g)

I. Take 10 g. of mortar lightly ground in mortar & pestle and digest in HCl (1+3) in a 250 ml beaker on a magnetic stirrer until all sand separates and settles at the bottom of beaker,
II. Filter all through two 2.5 micron filter paper, wash the beaker, filter paper, and all sand residue with dist. water,
III. Dry the residue at 110°C in an oven for 10 min., gently brush out from the filter paper and collect, then sieve the entire sand residue through No. 4 through 200 sieves in a mini sieve shaker (e.g., from Gilson),
IV. Determine the mass retained on each sieve, and on the pan (finer than No. 200 sieve),
V. Take photomicrographs of sand particles retained on each sieve for sand color variations in a stereomicroscope.

4. Acid & Alkali Digestion – Soluble Silica for Hydraulic Binder (5 g)

I. Grind 5-6 g of lightly ground fraction from mortar & pestle in a WC pulverizer for 30 sec.
II. Sieve thru. No. 50 sieve, collect the fraction passing the sieve,
III. Re-grind the residue retained on sieve for 15 sec. and mix thoroughly with the previous fraction;
IV. Use 5.000 g of thus prepared powder (passing No. 50 sieve) for digestion in 100 ml cold (3-5°C/38-41°F) HCl (1+4) in a 250 ml beaker for 15 min. on a magnetic stirrer,
V. Filter thru. two 2.5 micron filter paper and keep the filtrate# 1,
VI. Digest the residue with filter paper in 75 ml hot NaOH (below boiling) on hot plate for 15 min. on magnetic stirrer,
VII. Cool down to room temp. and filter thru. two 2.5 micron filter paper and collect filtrate# 2,
VIII. Combine these two filtrates, filter the combined filtrates thru. two 2.5 micron filter paper to remove any suspended silica (especially for sand-rich mortars, or if mortar is grounded too long); then dilute to 250 ml in a volumetric flask with dist. water, an aliquot (about 10 ml) is then used for XRF for soluble silica determination against the calibrations with standard PC mortars of known soluble silica contents prepared in the same way.

5. Acid Digestion – Acid-Insoluble Residue Content for Siliceous Sand Content (2 g)

I. Take 1-2 g of prepared mortar powder from Step 4 iii (passing No. 50 sieve) and digest in 50 ml HCl (1+3) in a 250 ml beaker (covered) on a hot pate rapidly near boiling, then 15 min. at a temp. below boiling, then cool down to room temperatures,
II. Filter thru. two pre-weighed 2.5 micron filter papers, washing the beaker, paper, and residue thoroughly with hot water,
III. Dry the filter paper at 110C for 10 min, cool in a desiccator to room temp. and measure the weight.
IV. Subtract from mass of dry filter paper to determine acid-insoluble residue content.

6. Chemical Analysis – Loss On Ignition for Free and Combined Water Content, and Carbonate plus Carbonation (2 g)

I. Take 1-2 g (W_1) of prepared mortar powder from Step 3 iii (passing No. 50 sieve) in a tarred porcelain crucible (keep a record of mass of the empty crucible),
II. Dry at 110°C for 15 min in a muffle furnace pre-set to 110°C, cool in a desiccator to room temp. and measure the mass (W_2) by subtracting the empty crucible mass from the total mass,
III. Ignite at 550°C for 15 min. in the muffle furnace pre-set to 550°C, cool in a desiccator to room temp. and measure the mass (W_3) by subtracting the empty crucible mass from the total mass,
IV. Ignite at 950°C for 15 min. in the muffle furnace pre-set to 950°C, cool in a desiccator to room temp. and measure the mass (W_4) by subtracting the empty crucible mass from the total mass,
V. Calculate the losses on ignition at 110°C, 550°C, and 950°C for free water, combined water, and carbonate plus degree of carbonation, respectively.

7. Mineralogy of Bulk Mortar, Extracted Sand, Extracted Binder, or Salt from XRD (at least 8 g)

I. Weigh 8.00 g of mortar (or extracted sand or binder as needed) lightly ground in a mortar & pestle, add three grinding/pelletizing aid tablets (e.g., from Oxford Instruments) and pulverize in a suitable mill to minimize contamination (e.g., Rocklab pulverizer with WC bowl or McCrone Micronizing Mill with agate) for 3 min. with anhydrous alcohol to get <45 micron size particles passing U.S. No. 325 sieve,
II. Take 6.8 to 7.0 g. of ground <45 micron prepared mass in an aluminum sample holder inside a stainless steel die to prepare a 32 mm pellet with 25 ton pressure for 1 min,
III. Use the prepared pellet for XRD and then use the same pellet for XRF.
IV. Do XRD on the binder-rich fraction, or salt either on a shallow-depth sample holder or preferably on a zero background quartz plate for small volume of sample.

8. Bulk Mortar's Composition from X-Ray Fluorescence (XRF) (same pellet used in XRD)

I. Use the same pellet prepared for XRD in the XRF, or, use a fused bead if sample volume is low to prepare a pellet. In either method, have calibrations of measured oxides with adequate standard.
II. XRF can also be used with proper calibrations for soluble silica determination on the filtrates after acid and alkali digestions, as described in Section 4.

9. Thermal Analyses (0.1 g), TGA, DTG, DSC, DTA, for quantitative analysis of various hydrous, sulfate, and carbonate phases in mortar, content of dolomitic lime added from the brucite content in mortar as determined from TGA or DSC, etc.

I. Simultaneous TGA and DSC analyses can be done on 30-70 mg of finely ground (<0.6 mm) mortar in alumina crucible (70 µl, no lid) from 30°C to 1000°C at a heating rate of 10°C/min with high purity nitrogen as purge gas at a flow rate of 75.0 ml/min .

10. Infrared Spectroscopy, for determination of various organic additives, paint, and clays in mortar

I. Take an aliquot of powder prepared for thermal analysis, or peel a paint and use that in Universal ATR of FTIR.
II. Alternately, digest a pulverized mortar in acetone to extract the organic additive and analyze the liquid in FTIR for characteristic functional groups.

11. Ion Chromatography of Water-Soluble Salts (1 g)

I. Take an aliquot of 1.00 gram powder prepared for chemical analysis (i.e. passing U.S. No. 50 sieve), digest in hot (below boiling) 50 ml distilled or deionized water for at least 6 hours in a beaker on a magnetic stirrer covered with watch glass, filter the solid residues out to collect the filtrate and analyze the final 100 ml of filtrate for soluble salts (chloride, sulfate, nitrate, nitrite, phosphate, etc.) by ion chromatography.

Figure 4: Outline of step-by-step procedures of various laboratory analyses of a masonry mortar. FTIR was not needed for the present mortar sample.

RESULTS

Grain-size Distribution of Sand

Figure 5 shows grain-size distribution of sand extracted after a series of digestion of mortar in dilute (1+3) hydrochloric acid. Also shown are stereo-photomicrographs of sand particles retained on various sieves including size, shape, angularity, and color variations of sand particles. Note varied color tone of majority of sand particles. A few particles retained on Nos. 30 and 50 are still agglomerated due to incomplete separation of binder from sand despite repeated acid digestion. It is important to remember that argillaceous sand particles, if any, have broken down during acid digestion and hence are present mostly in the finest fractions instead of intact grains, and calcareous particles, if present, are mostly dissolved out in acid. Hence, photos of particles retained on each sieve are mostly from the siliceous component of sand.

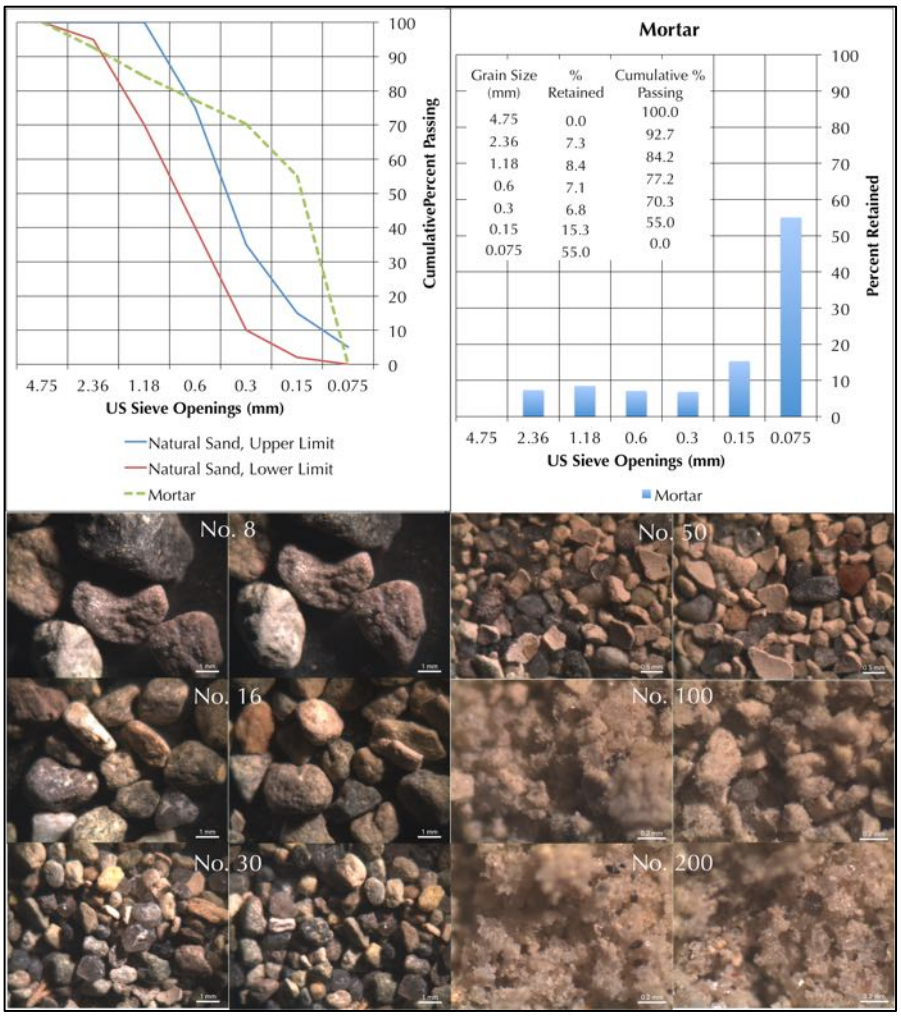

Figure 5: Grain-size distribution of sand extracted from the mortar after acid digestion. In the top left plot, size distirbution of sand is compared with upper and lower limit of natural sand in ASTM C 144 (blue and red lines). Top right plot shows distribution of sand (inset Table shows percetn retained and cumulative percent passing through each sieve). Bottom photos show stereo-photomicrographs of sand particles retained on various sieves.

Size distribution of sand in the mortar is compared with the ASTM C 144 specification of natural sand for unit masonry, which shows that for all size fractions, sand is noticeably finer than the upper and lower limits of ASTM C 144 size gradation for natural sand. The 'percent retained' histogram plot shows size distribution and enrichment in finest size fraction of sand. Therefore, sand is judged to be not in conformance to a modern ASTM C 144 masonry sand but much finer than modern sand.

Subsequent optical microscopical examinations of sand determined its **volcanic basalt and siliceous (quartz, quartzite, granite, chert) – calcareous (limestone) sand composition**. Therefore, sand extracted from acid digestion is determined to be the basalt and siliceous portion of sand while the limestone component in sand was dissolved away in acid and hence results provided here are representative of the siliceous part of sand.

Optical Microscopy of Sand

Figure 6 shows lapped cross sections (top row) and photomicrographs of lapped cross sections of mortar taken from a reflected-light Stereozoom microscope to show the overall size, shape, color variations, distribution, gradation, and compositions of sand in the mortar, color and appearance of interstitial binder, and air voids. Sand particles are less than 2 mm in nominal size (consistent with 100 percent particles passing through 4.75-mm sieve openings in Figure 5), subangular to subrounded, mostly equidimensional to a few elongated in shape, and appear in varied color ranges from dark gray to light brown and light gray, as seen in the photos.

Figure 7 shows crossed polarized-light views of photomicrographs of the blue dye-mixed epoxy-impregnated thin section of mortar (Figure 3) viewed in a transmitted-light Stereozoom microscope. Sand particles show volcanic rocks and minerals (consisting of basalt, and basaltic plagioclase feldspar), along with major amounts of quartz, quartzite, granite, chert, subordinate amounts of limestone, and minor amounts of sandstone, mafic minerals, etc., thus indicating an overall mixed **volcanic (basaltic) and siliceous-calcareous composition of sand,** which is probably derived from the Walnut Canyon, which lies on the Colorado Plateau and cuts through the Permian Kaibab Limestone and Coconino Sandstone.

Interstitial paste between sand grains shows typical ultrafine, porous, severely carbonated nature of a lime mortar but with occasional residual Portland cement particles indicating use of binders having abundant lime and subordinate cement components, where abundant lime in the original binder is responsible for the overwhelming porous, ultrafine-grained severely carbonated appearance of paste, whereas a subordinate cement component in the binder has provided occasional residual cement particles with associated localized denser paste from cement hydration and carbonation. All these features are characteristic of a historic high-lime cement-lime mortar made using lime, most probably added as lime putty (which shows occasional white lumps of lime, e.g., arrows in Figure 6), mixed with subordinate cement (probably coarsely ground to leave residual cement particles to be identified), and river sand.

Figure 8 shows black-and-white binary images of: (a) the mosaic of plane-polarized light photos of thin section from a transmitted-light Stereozoom microscope (left) to highlight (b) the void spaces and shrinkage microcracks in blue in the left and correspondingly black in the middle photo, and (c) sand particles in black against everything else in white in the right.

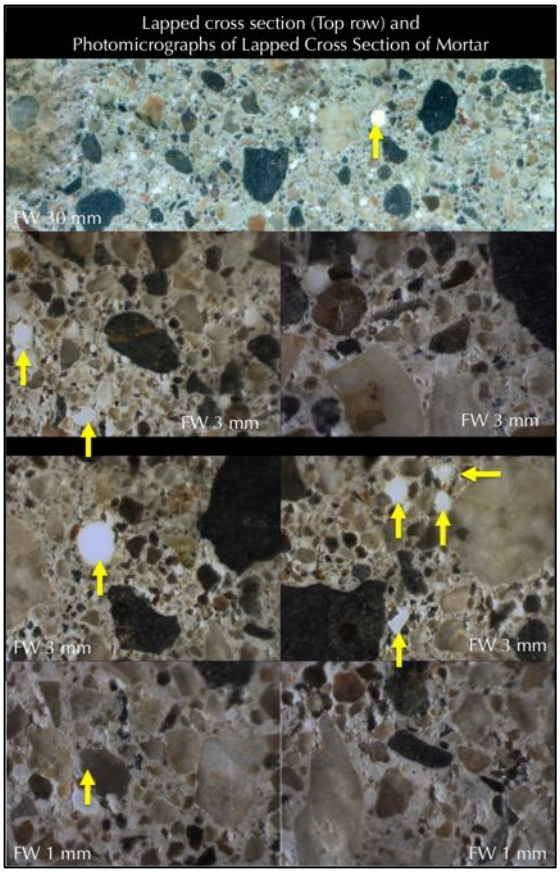

Figure 6: Photomicrographs of lapped cross section of mortar. Arrows show some white lime lumps. FW = Field Width

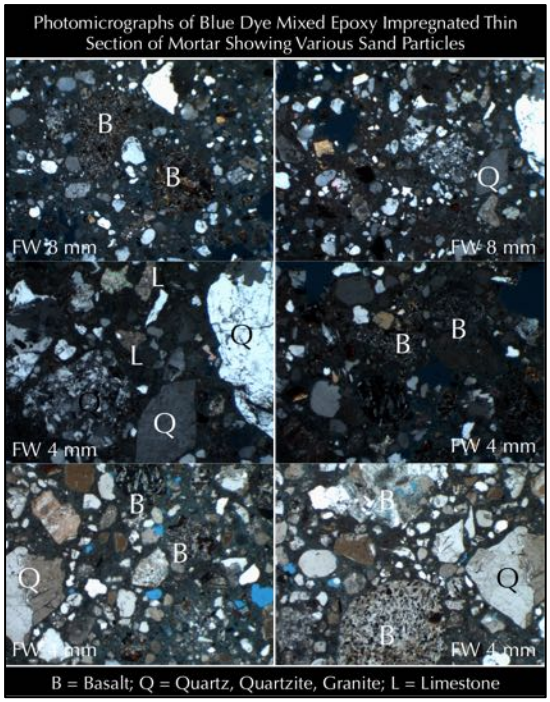

Figure 7: Plane polarized light photomicrographs of thin section of mortar taken from a transmitted-light Stereozoom microscope. FW = Field Width

Image analyses of these binary images (by Image J, from the National Institute of Health, www.imagej.nih.gov) provided a *rough estimate* of 2.1 percent void spaces, which are mostly the coarse voids (actual air content is estimated to be 4 to 6 percent) and shrinkage microcracks consistent with non-air-entrained nature of the mortar, and, 38.8 percent sand by area.

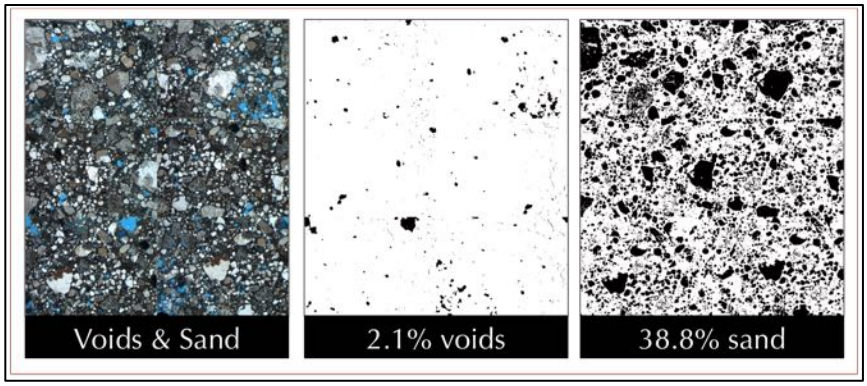

Figure 8: Binary image analyses of voids and sand.

Figure 9 shows photomicrographs of thin section of mortar from transmitted-light petrographic microscope, which show volcanic rocks and minerals (consisting of basalt, and basaltic plagioclase feldspar), along with major amounts of quartz, quartzite, granite, chert, subordinate amounts of limestone, and minor amounts of sandstone, mafic minerals, etc., thus indicating an overall mixed **volcanic (basaltic) and siliceous-calcareous composition of sand**.

Sand particles are mostly derived from the Walnut Canyon having volcanic (basalt), siliceous (quartz, quartzite, chert, sandstone), and calcareous (limestone) components all derived from the canyon rocks.

Sand particles are present in sound condition without any potentially deleterious reactions (e.g., alkali-aggregate reactions). Soundness of sand is another testament of use of a natural sand that was durable during service in the mortar.

Based on these observations, sand for the mix for replacement mortar in renovation can be used from the local canyon source after conducting a petrographic examination of the sand to be used *a la* ASTM C 295 to confirm the match with the sand found in this examined mortar.

Intricate details in all optical photomicrographs in Figures 6, 7, 9, 10, and 11 can be best viewed by enlarging these pages. In Figures 9 and 10, PPL and XPL stands for observations in plane and crossed polarized light modes, respectively in a petrographic microscope.

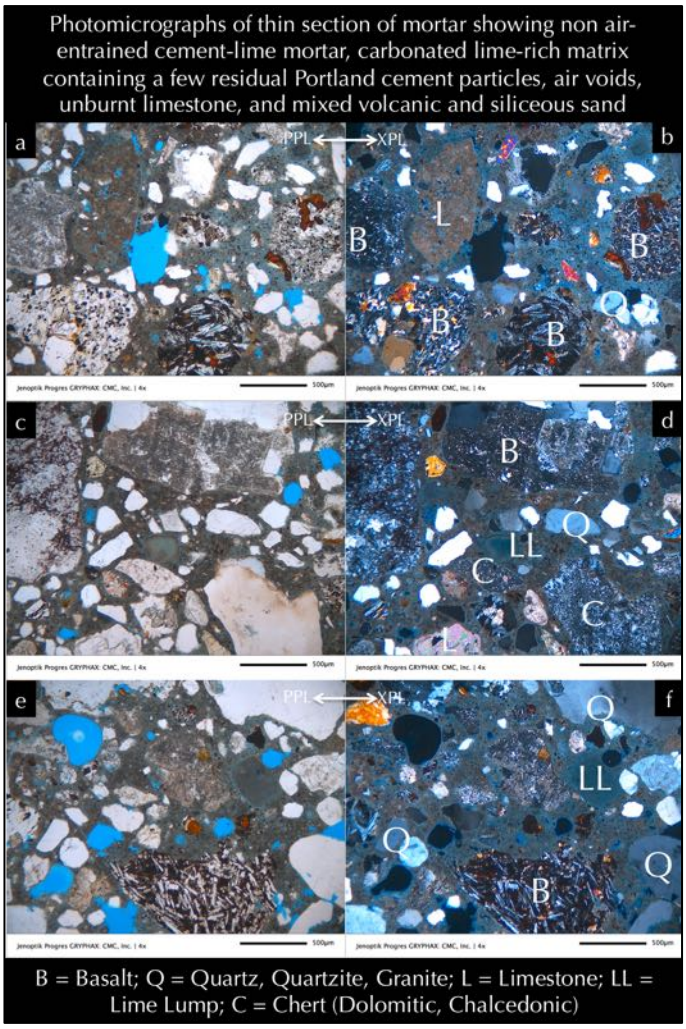

Figure 9: Mortar sand as seen through petrographic microscope. Sand consists of mainly volcanic sand (basalt) and siliceous (quartz, quartzite) sand particles, mostly subangular to well-rounded, well-graded, and well-distributed. PPL = Plane-polarized light and XPL = Crossed-polarized light modes in a petrographic microscope.

Optical Microscopy of Paste

Figures 10 and 11 provide photomicrographs of the interstitial matrix phases of paste between sand particles to characterize the compositions and microstructure of binder as revealed from photomicrographs of thin section of mortar in a petrographic microscope.

Figure 10 shows porous, fine-grained severely carbonated nature which is typical of many historic lime mortars but with occasional residual Portland cement grains, which are characteristic of use of binder having abundant lime mostly added as lime putty but mixed with a subordinate amount of Portland cement.

Figure 11 shows contrasting porosities and densities of paste between denser cement hydrated areas around residual cement particles and more porous and carbonated lime-rich areas in the matrix that are characteristic of use of a high-lime lime-cement mortar.

Figure 11 shows plane polarized light views of thin section images depicting residual and relict Portland cement particles with characteristic texture of subhedral alite and anhedral belite in dark interstitial ferrite matrix scattered in variably carbonated lime-cement matrix, as well as minor amount of spherical fly ash particles, indicating use of a blended cement as the hydraulic component of binder.

Within the paste areas in Figures 10 and 11 are: (a) residual Portland cement, (b) areas of cement hydration products, (c) fine spherical clear to light to dark brown to black fly ash particles, (d) overwhelming areas of carbonation of lime, (e) occasional lime lumps – all carrying a taletell feature of a historic high-lime blended Portland cement plus fly ash-lime mortar.

Based on optical microscopy alone, therefore, the mortar is determined to have a lime-cement-sand based composition made using lime putty, subordinate Portland cement, and sand of volcanic basalt-plagioclase and natural siliceous (quartz, quartzite, granite) - calcareous (limestone) composition. The lime component was derived from calcination of calcitic limestone, whereas Portland cement component was derived from calcination of limestone-shale mixture, which were perhaps ground coarsely compared to modern-day Portland cement.

Subsequent SEM-EDS studies of paste determined the dolomitic lime composition of lime (from high magnesia content in paste in SEM-EDS studies) to indicate calcination of a dolomitic limestone for the lime putty component in the mortar.

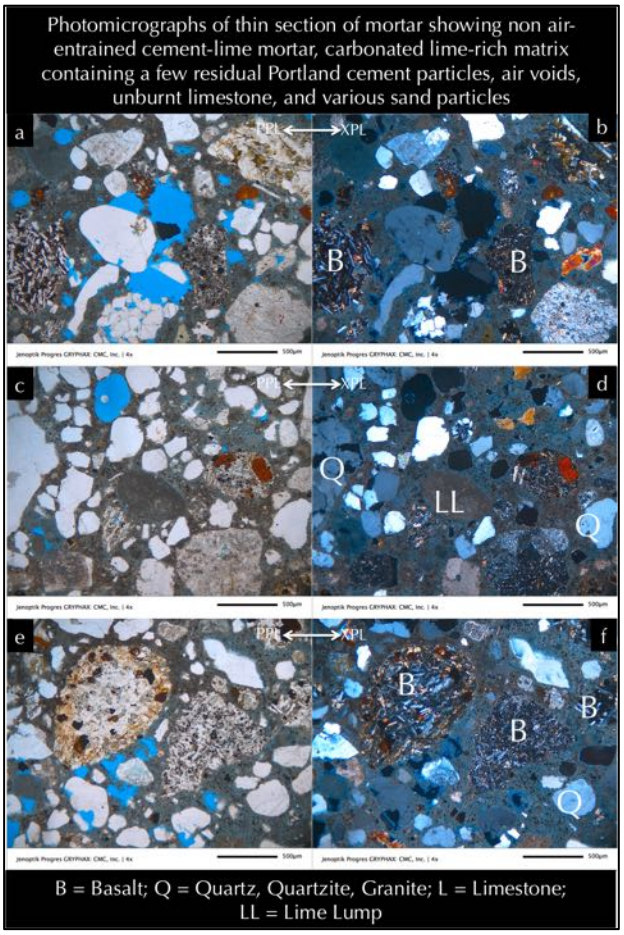

Figure 10: The lime-Portland cement paste.

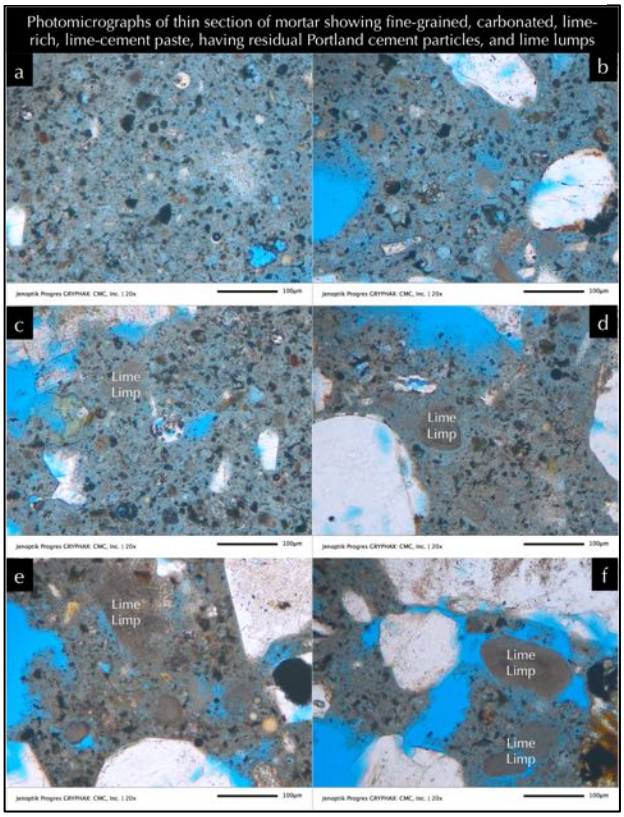

Figure 11: Details of microstructure of paste.

Paste Compositions and Microstructure From SEM-EDS

Figure 12 shows backscatter electron image (BSE), secondary electron image (SED), and X-ray elemental maps (bottom) of thin section of mortar from in a scanning electron microscope.

BSE image shows sand particles that appear in medium gray with sharp boundaries, and paste in variable shades of gray from porous areas in darker tones than the denser and carbonated areas.

In X-ray elemental maps, siliceous sands are highlighted in Si-map, calcareous (lime) paste is highlighted in Ca-map, feldspar grains in sand are highlighted in Na, K, Al, and Si maps. Enrichment of calcium in paste in Ca-map and magnesium in Mg-map indicate use of a dolomitic lime in the binder.

Figure 13 shows compositional analyses of paste at various areas (at the tips of callouts) carefully selected to avoid any interference from sand particles or residual Portland cement particles. Results of paste compositions are provided in the Table beneath.

Average paste composition after filtering interference from sand or cement particles in Figure 14 Table showed about 70% lime, 20% silica, 4% alumina, 1.4 percent magnesia, and 3.8% iron oxide (as FeO). Magnesia content indicates use of a dolomitic lime binder.

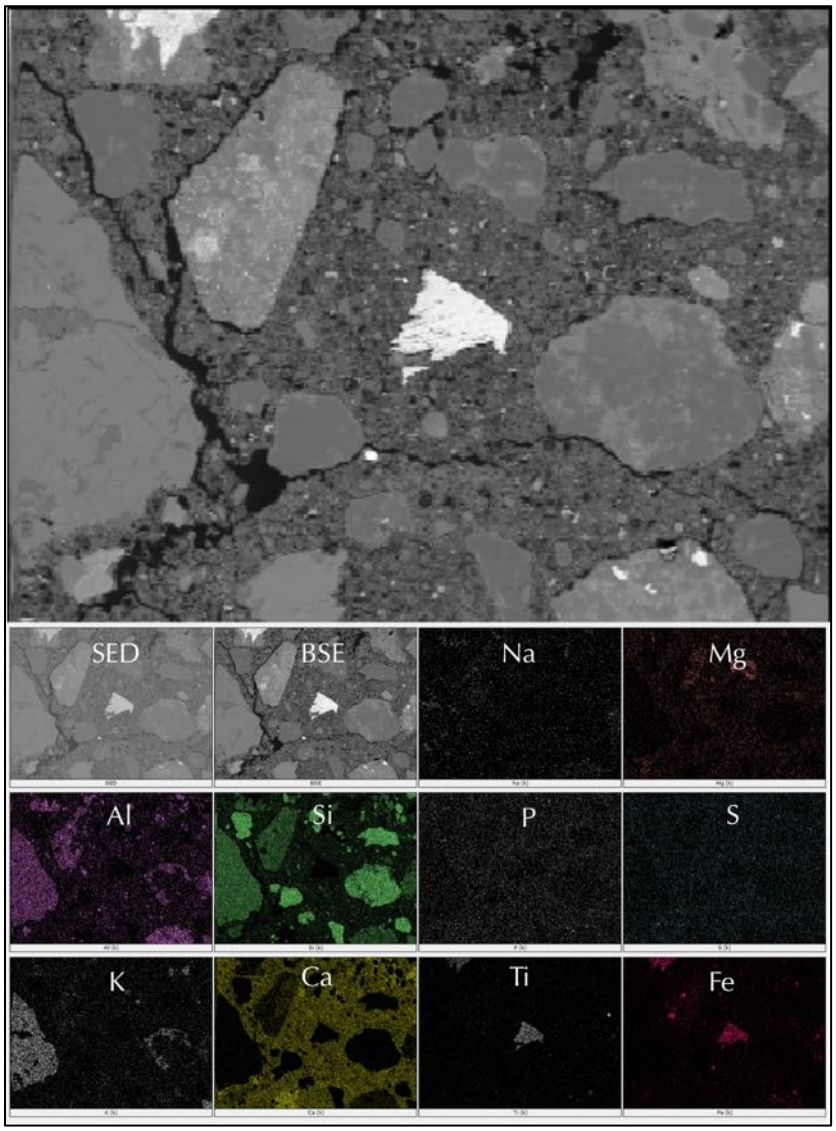

Figure 12: Backscatter electron image (top and bottom marked as BSE), corresponding secondary electron image SED and X-ray elemental maps of mortar.

The cementation indices (CI) of paste in Figures 13 and 14 are calculated after Eckel (1922) as CI = $[(2.8*SiO_2)+(1.1*Al_2O_3)+(0.7*\ Fe_2O_3)]/[(CaO)+(1.4*MgO)]$, which measures relative hydraulicity of paste e.g., non-hydraulic lime pastes have very low CI (< 1) compared to Portland cement pastes (CI is >1). Results show an average CI of 0.43, which is characteristic of a lime binder that has an inherent hydraulicity, or, a cement-lime binder of high lime content – where latter is found to be the case from optical microscopy. CI varied across the paste depending on degree of mixing of cement and lime components and subsequent hydration and carbonation of components followed by degree of alterations (carbonation, leaching, etc.) that have caused some variations in major oxide contents of paste. The average CI value provides a fair representation of use of a high-lime lime-cement binder, which, is consistent with the observations from optical microscopy.

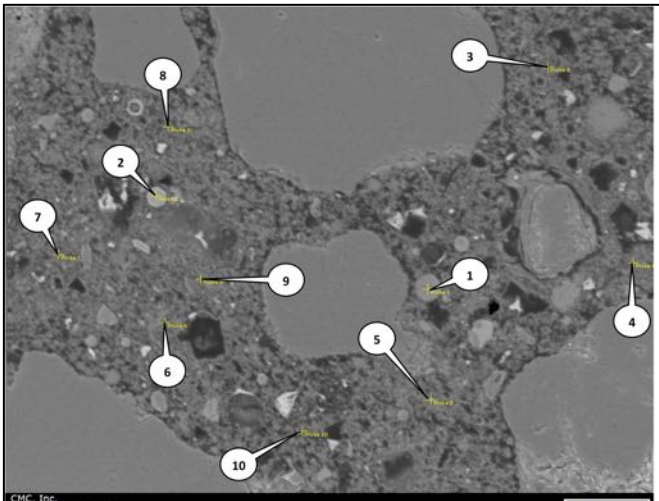

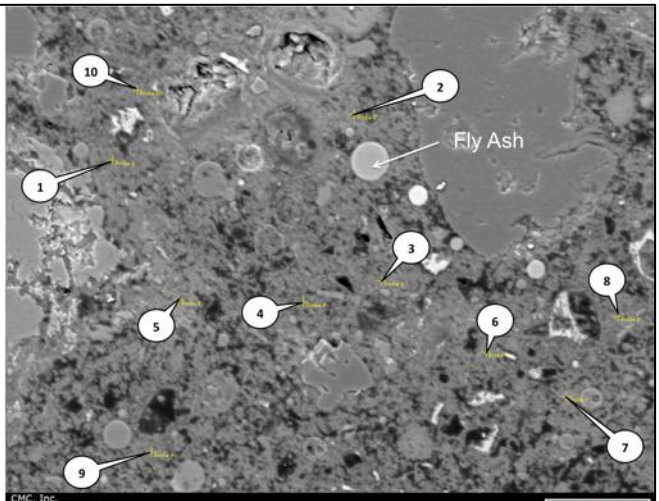

Probe	CaO	SiO_2	Al_2O_3	Na_2O	MgO	SO_3	K_2O	TiO_2	FeO	Total	Phase	Paste CI
1	7.07	54.66	23.93	0.00	0.45	0.00	2.67	2.30	8.93	100.01	Fly Ash	-
2	5.41	40.04	22.43	0.00	0.19	0.00	1.35	2.55	28.02	99.99	Fly Ash	-
3	53.46	15.97	9.98	0.00	1.08	0.00	0.81	1.04	17.65	99.99	Paste	1.24
4	64.74	21.44	5.26	0.00	1.53	0.00	0.94	0.26	5.83	100.00	Paste	1.05
5	75.66	17.28	3.43	0.00	1.14	0.00	0.57	0.13	1.80	100.01	Paste	0.69
6	62.82	23.74	5.61	0.00	2.17	0.00	1.32	0.57	3.77	100.00	Paste	1.14
7	30.43	42.45	16.24	0.00	0.62	0.00	2.70	1.88	5.67	99.99	Feldspar	4.50
8	76.14	17.13	3.87	0.00	1.38	0.00	0.00	0.00	1.47	99.99	Paste	0.68
9	65.57	22.41	5.13	0.00	0.98	0.00	1.12	0.97	3.83	100.01	Paste	1.06
10	0.00	98.97	0.56	0.00	0.00	0.00	0.32	0.01	0.13	99.99	Quartz	-
Average	66.40	19.66	5.55	0.00	1.38	0.00	0.79	0.50	5.73	100.00	Paste	0.98
St. Dev.	8.54	3.26	2.33	0.00	0.44	0.00	0.47	0.44	6.05	0.01		0.23

Probe	CaO	SiO_2	Al_2O_3	Na_2O	MgO	SO_3	K_2O	TiO_2	FeO	Total	Phase	Paste CI
1	70.66	21.11	3.40	0.01	1.42	0.00	0.41	0.01	2.98	100.00	Paste	0.89
2	79.11	13.04	1.02	0.01	0.01	0.00	0.86	2.32	3.62	99.99	Paste	0.51
3	69.45	20.40	2.40	0.01	2.03	0.00	0.58	0.25	4.88	100.00	Paste	0.87
4	67.50	23.61	3.60	0.01	1.61	0.00	0.32	0.79	2.56	100.00	Paste	1.03
5	64.17	23.62	7.06	0.01	0.31	0.00	0.64	0.16	4.02	99.99	Paste	1.19
6	67.67	22.42	4.41	0.01	2.73	0.00	0.46	0.01	2.30	100.01	Paste	0.97
7	81.05	15.63	2.70	0.01	0.01	0.00	0.14	0.01	0.45	100.00	Paste	0.58
8	75.16	17.06	2.44	0.01	2.07	0.00	0.00	0.76	2.50	100.00	Paste	0.67
9	25.89	41.80	12.59	0.00	4.63	0.00	3.98	0.74	10.36	99.99	Grain	-
10	73.11	19.76	3.20	0.01	2.25	0.00	0.35	1.31	0.01	100.00	Paste	0.77
Average	71.99	19.63	3.36	0.01	1.38	0.00	0.42	0.62	2.59	100.00	Paste	0.83
St. Dev.	5.62	3.68	1.68	0.00	1.03	0.00	0.26	0.78	1.57	0.01		0.22

Figure 13: Backscatter electron images (top row) and major element oxide compositions and CIs of paste in left and right photos measured at the tips of callouts across several areas of paste. Notice some spherical fly ash particles in the right photo, some of which are analyzed in the left photo to confirm the typical aluminosilicate composition of fly ash.

Figure 13 shows some spherical fly ash particles in paste having typical aluminosilicate composition of fly ash particles that are indicative of use of a blended cement as the hydraulic component in the binder having major amount of Portland cement and minor amount of fly ash.

Figure 14 shows a systematic trend in variations of lime and silica contents of paste with paste-CI (Eckel, 1922) where lime-rich, low-CI areas of paste represent carbonated products of lime, whereas silica-rich, high-CI areas represent higher hydraulicity from hydration products of Portland cement. Continuous linear trends in these plots are the consequence of mixing a hydraulic (Portland cement) and less or non-hydraulic (dolomitic lime) components in the binder. Similar trends are found in modern cement-lime mortars as well, prepared by mixing Portland cement (hydraulic) and hydrated lime or lime putty (non-hydraulic) components.

SEM-EDS results are consistent with the optical microscopical observations of an overall high-lime dolomitic lime and Portland cement based compositions of the original binder where lime was made using calcination of a dolomitic limestone, and was added with Portland cement as two essential binders to provide the necessary hydraulicity and water retention properties of mortar.

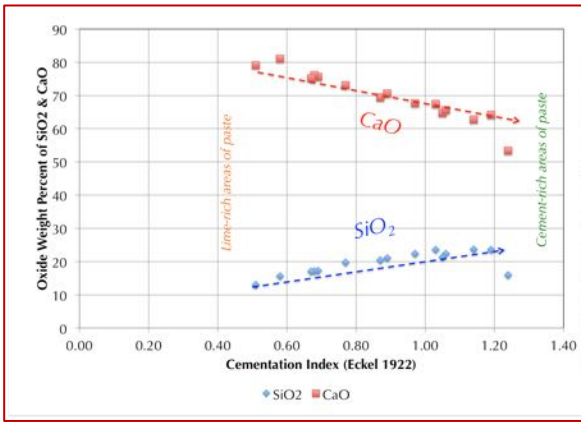

Compositions of Lime-Cement Paste Plotted in the Graph

Data	CaO	SiO2	Al2O3	Na2O	MgO	SO3	K2O	TiO2	FeO	Total	Phase	Paste CI
1	53.46	15.97	9.98	0.00	1.08	0.00	0.81	1.04	17.65	99.99	Paste	1.24
3	64.74	21.44	5.26	0.00	1.53	0.00	0.94	0.26	5.83	100.00	Paste	1.05
5	75.66	17.28	3.43	0.00	1.14	0.00	0.57	0.13	1.80	100.01	Paste	0.69
6	62.82	23.74	5.61	0.00	2.17	0.00	1.32	0.57	3.77	100.00	Paste	1.14
7	76.14	17.13	3.87	0.00	1.38	0.00	0.00	0.00	1.47	99.99	Paste	0.68
9	65.57	22.41	5.13	0.00	0.98	0.00	1.12	0.97	3.83	100.01	Paste	1.06
10	70.66	21.11	3.40	0.01	1.42	0.00	0.41	0.01	2.98	100.00	Paste	0.89
11	79.11	13.04	1.02	0.01	0.01	0.00	0.86	2.32	3.62	99.99	Paste	0.51
12	69.45	20.40	2.40	0.01	2.03	0.00	0.58	0.25	4.88	100.00	Paste	0.87
13	67.50	23.61	3.60	0.01	1.61	0.00	0.32	0.79	2.56	100.00	Paste	1.03
14	64.17	23.62	7.06	0.01	0.31	0.00	0.64	0.16	4.02	99.99	Paste	1.19
15	67.67	22.42	4.41	0.01	2.73	0.00	0.46	0.01	2.30	100.01	Paste	0.97
17	81.05	15.63	2.70	0.01	0.01	0.00	0.14	0.01	0.45	100.00	Paste	0.58
18	75.16	17.06	2.44	0.01	2.07	0.00	0.00	0.76	2.50	100.00	Paste	0.67
19	73.11	19.76	3.20	0.01	2.25	0.00	0.35	1.31	0.01	100.00	Paste	0.77
Average	69.75	19.64	4.23	0.01	1.38	0.00	0.57	0.57	3.84	100.00	#DIV/0!	0.89
Stn. Dev.	7.22	3.40	2.19	0.01	0.82	0.00	0.39	0.65	4.13	0.01	#DIV/0!	0.23

Figure 14: Variations of lime and silica contents of paste with CI after Eckel (1922). Paste compositions are screened here compared to results in Figure 13 to remove any interference from sand or residual cement particles.

Air

Figure 15 shows photomicrographs of lapped cross section of mortar (left) and blue dye-mixed epoxy-impregnated thin section (right) both showing no entrained air and a few coarse near-spherical and irregularly-shaped entrapped air voids that are highlighted by blue epoxy in the right photo and indicate use of a non-air-entrained mortar, which is common in most historic mortars.

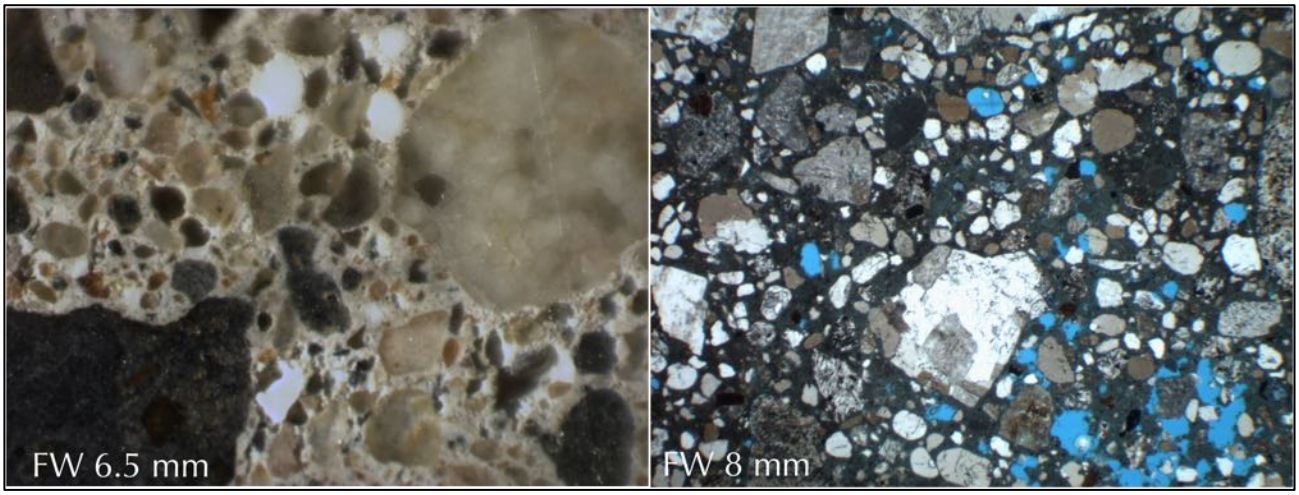

Figure 15: Photomicrographs of lapped cross section (left) and blue dye-mixed epoxy-impregnated thin section (right) of mortar showing very few entrapped air voids that are highlighted by blue epoxy in right photo and indicate use of a non-air-entrained mortar, which is common in most historic mortars. FW = Field Width.

Mineralogy of Mortar From XRD

Figure 16 shows X-ray diffraction pattern of the mortar, and quantitative analysis (Rietveld) of major mineralogical compositions of mortar consisting of 62.1% quartz as the dominant mineral from sand, 13.5% calcite from carbonated paste, and 17.4% plagioclase (albite) feldspar from sand. XRD analysis did not find any potentially deleterious salt in the mortar.

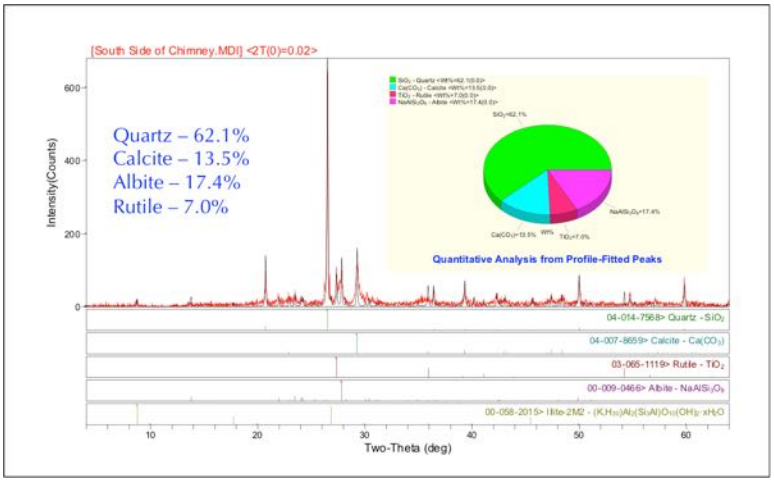

Figure 16: X-ray diffraction pattern of mortar showing quartz, and albite as the main mineral phases from volcanic sand, rutile in sand, calcite as the other main phase from carbonated cement-lime paste.

Composition of Mortar From XRF (Major Element Oxides), Acid & Alkali Digestion (Soluble Silica), Loss on Ignition (Free Water, Combined Water, Carbonation), and Acid-Insoluble Residue Content (Siliceous Sand Content)

Table 1 shows oxide compositions of mortar determined from pressed pellet of pulverized (< 45 micron size) bulk mortar in XRF. Silica is contributed from sand, cement, and fly ash. Lime is contributed from carbonated paste. Alumina, iron, and alkalis are contributed from both sand and paste. Balance includes volatiles (combined H_2O, CO_2) not measured in XRF.

Mortar Composition	Values	Methods
Silica - SiO_2	49.2	XRF
Alumina - Al_2O_3	7.18	XRF
Iron - Fe_2O_3	4.27	XRF
Lime - CaO	15.9	XRF
Magnesia - MgO	3.56	XRF
Sodium - Na_2O	1.59	XRF
Potassium - K_2O	0.951	XRF
Titanium - TiO_2	0.568	XRF
Phosphorus - P_2O_5	0.253	XRF
Sulfate - SO_3	ND	XRF
Balance	16.6	XRF
Total	100	XRF
Soluble Silica in filtrates of Cold-HCl and Hot-NaOH digested mortar	0.15	XRF
Acid-Insoluble Residue	68.85	Gravimetry
Loss on Ignition @ 110°C	1.20	Gravimetry
Loss on Ignition @ 550°C	1.90	Gravimetry
Loss on Ignition @ 950°C	8.80	Gravimetry

Table 1: Bulk oxide compositions and soluble silica content of mortar from XRF, and acid-insoluble residue content and losses on ignition from gravimetry.

Portland cement was responsible for the detectable soluble silica in the XRF analysis of filtrate after digestions in cold-HCl and hot-NaOH.

Acid-insoluble residue content of mortar is determined after digesting pulverized (<0.3 mm size) fragments of mortar in hydrochloric acid. Losses on ignition of a separate aliquot of pulverized mortar to 110°C, 550°C, and 950°C correspond to free water, combined (hydrate) water, and degree of carbonation, respectively. Due to the presence of siliceous rocks in the sand (as determined from petrography) as the major component, the determined acid-insoluble residue content (68.85 percent) closely corresponds to the sand content in the mortar. The loss on ignition at 550°C corresponds to the water content from dehydration of Portland cement plus fly ash paste. The loss on ignition at 950°C corresponds to degree of carbonation of carbonated lime and cement paste. The highest loss at 950°C is consistent with the high-lime hence abundant carbonated lime composition of paste in the mortar.

Thermal Analyses

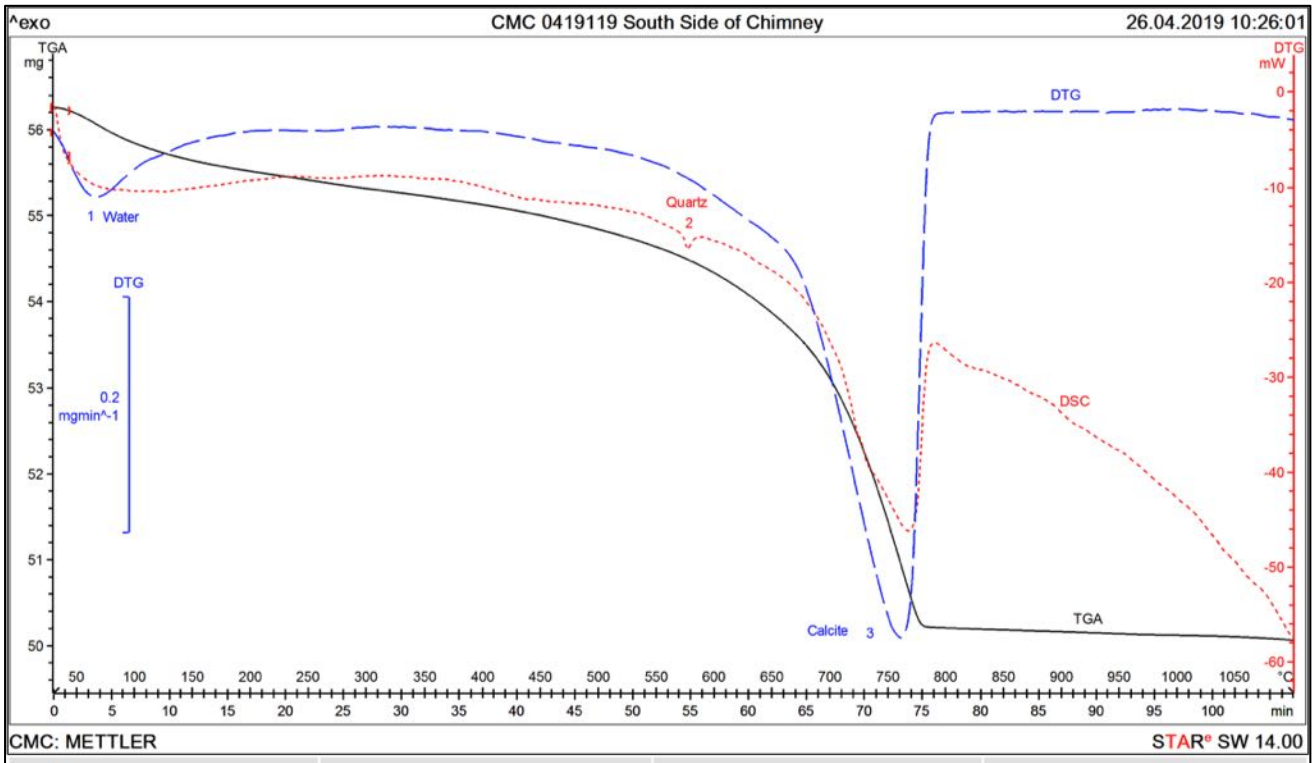

Peak#	Peak Position (°C)	Phase	Amount (%)
1 (DTG)	62.47	Water	1.02
2 (DSC)	575.52	Quartz	33.25
3 (DTG)	759.17	Calcite	11.89

Figure 17: Thermal analyses of mortar.

Figure 17 shows TGA (in bold black), DSC (in dotted red), and DTG (in dashed blue) curves of mortar showing losses in weight due to decompositions (loss of water and carbon dioxide) of various phases during controlled heating in a Mettler-Toledo's simultaneous TGA/DSC 1 unit from 30ºC to 1000ºC in a ceramic crucible (alumina 70µl, no lid) at a heating rate of 10ºC/min in a nitrogen purge at a rate of 75 mL/min.

Dehydration and decarbonation reactions are marked as endothermic peaks in the DTG curve, whereas alpha to beta-form polymorphic transition of quartz is marked at the characteristic temperature of 573 ºC in the DSC curve.

In the DTG curve, successive losses in weights are detected at (i) 62.47 (Peak# 1) from loss of water, and (ii) 759.17ºC (Peak# 3) from carbonation of fine-grained calcite in carbonated lime paste. DSC curve shows polymorphic transition from alpha to beta form of quartz at 575.52ºC from silica (quartz) sand (Peak# 2). Quantitative estimates of quartz and calcite are determined to be 33.2 and 11.9 percent, respectively.

High calcite content is consistent with severely carbonated nature of the mortar from its high-lime composition. Results of thermal analyses are therefore consistent with the results obtained from microscopy and XRD studies.

Ion Chromatography

Figure 18 shows chromatogram of water-soluble salts in mortar after digesting a gram of pulverized mortar in distilled water for 30 minutes at a temperature below boiling, followed by continued digestion in water at the ambient laboratory condition for 24 hours. The filtrate was analyzed by ion chromatography. Results showed negligible chloride (0.014%) and sulphate (0.064%), probably from mortar's ingredients with no evidence of any deleterious salts from the environment.

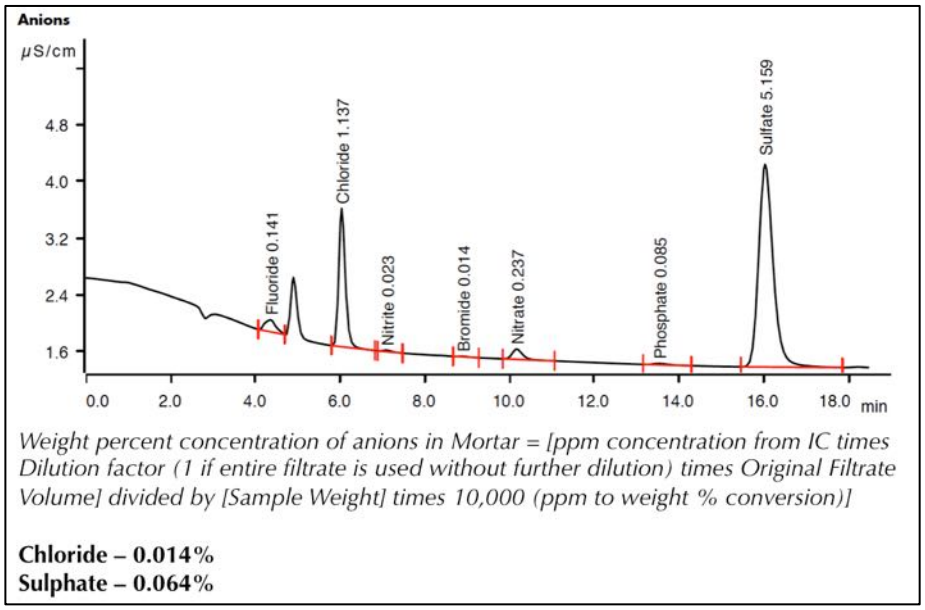

Figure 18: Chromatogram of water-soluble anions in mortar.

DISCUSSIONS

Type of Mortar & Its Ingredients

Optical microscopy has determined the high-lime cement-lime-volcanic/siliceous/calcareous sand composition of the historic mortar from its: (a) characteristic mineralogies of sand and binder, (b) hydrated and carbonated microstructure and composition of paste having an overwhelming porous, ultrafine, severely carbonated lime microstructure with scattered residual Portland cement particles, minor spherical fly ash particles, and associated occasional denser carbonated paste of cement hydration products, and (c) mixed volcanic (basalt, plagioclase feldspar), siliceous (quartz, quartzite, chert, granite, sandstone), calcareous (limestone) compositions. Sand particles are mostly derived from the Walnut Canyon having volcanic, siliceous, and calcareous components all derived from the canyon rocks. SEM-EDS analyses of paste has confirmed the presence of high-lime dolomitic lime and Portland cement binder components where lime has a magnesian lime composition, which have provided an average paste-cementition index, CI (after Eckel 1922) of 0.89. XRD analysis has confirmed the dominance of quartz from silica sand, subordinate presence of albite feldspar from sand, and abundant calcite from carbonated lime paste and calcareous (limestone) component of sand. XRF studies of acid and alkali-digested filtrates of mortar showed detectable soluble silica from Portland cement component of binder to confirm the lime-cement composition. Predominant endothermic peak from calcite decarbonation in thermal analyses, and high magnesium composition of paste are consistent with use of a dolomitic lime component in the binder, which was probably added as a lime putty where quicklime was manufactured from calcination of a dolomitic limestone. Results obtained from microscopy, chemical analyses, and finally thermal analyses are all consistent, confirmatory to each other, and provided a comprehensive understanding of mortar, which was determined to be prepared from mixing major amount of dolomitic lime putty with subordinate amount of blended (Portland+fly ash) cement, and Walnut Canyon sand.

Mix Calculations

Information obtained from: (a) chemical analyses of mortar to determine the soluble silica content, water contents, and insoluble residue content, and, (b) determination of use of a high-lime Portland cement plus fly ash and dolomitic lime based binder composition of mortar from microscopy and chemical analyses - are used to calculate the lime and cement contents, sand content, and, eventually, the volumetric proportions of ingredients

of mortar. Due to the presence of fly ash along with Portland cement, the soluble silica content of mortar has contributions from both cement and fly ash where conventional (ASTM C 1324) method of calculation of mix proportion of a modern cement-lime mortar cannot be used without knowing the soluble silica content of fly ash.

a. Since the sand is determined to be siliceous (quartz-quartzite-feldspar-chert) and calcareous (limestone) sand, where the limestone component is found to be present only at a minor amount from optical microcopy, the sand content is determined mainly from the siliceous component from the hydrochloric acid-insoluble residue content in the mortar. Sand content is thus determined to be 68.85 percent.
b. The binder is found to have major amount of dolomitic lime and subordinate amount of blended cement (of Portland cement plus fly ash) from optical microscopy and SEM-EDS studies of paste. Assuming about 29 percent MgO in a typical dolomitic lime, the average 1.4 percent MgO content of paste from SEM-EDS gives about 4.8 percent dolomitic lime by mass. This calculation assumes no contribution of MgO from cement or sand to the paste besides dolomitic lime.
c. The cement plus fly ash content is then calculated from soluble silica content of mortar and an assumption of soluble silica contents of cement and fly ash, which is approximately 10.1 percent.
d. Volumetric proportions of blended cement, lime, and sand are calculated from corresponding dry densities of 94 (which is common for Portland cement, since fly ash is found to be present only at a minor amount, this value is used for blended cement as well), 40, and 80 lbs./ft^3, respectively. Volumetric proportions of blended cement-to-lime-to-sand are thus calculated to be, 0.107-to-0.120-to-0.860, or **1-part cement to 1.12 part lime to 8.0-part sand (i.e. 3.8-times sand than sum of blended cement and lime components)**.
e. Therefore, the volumetric proportions of cement, lime, and sand are calculated to be **1-part blended cement to 1.1-part dolomitic lime, to 8-part sand, which is closely equivalent to a modern day ASTM C 270 Type N cement-lime mortar.** Result of this calculation confirms microstructural observation of a high lime blended cement-dolomitic lime mortar observed from optical and electron microscopy.

Condition

No potentially deleterious chemical or physical deterioration of mortar was found, e.g., lime leaching or freezing-related distress. Sand used was present in sound condition without any deleterious reactions with the binder. Based on mix calculations, however, the mortar is found to be over-sanded compared to ASTM C 270 specified mortars for use in unit masonry. Paste showed normal characteristics of a historic high-lime blended cement-dolomitic lime composition of paste without any unusual cracking (other than some normal shrinkage-related microcracking from carbonation of lime pastes), or loss of integrity (increased porosity) from leaching. Ion chromatography of water-soluble anions from the mortar did not detect any potentially deleterious salt as a contaminant. Overall the mortar is found to be present in fairly sound condition without any chemical or physical deterioration to interfere with the long-term performance of the masonry.

Replacement Mix For Mortar

Based on: (i) the determined high-lime blended cement-dolomitic lime binder composition of mortar from microscopy and chemical analyses; (ii) natural siliceous-calcareous sand compositions of aggregate; and (iii) calculated volumetric proportions of 1-part cement to 1.1-part lime to 8.0-part sand, a possible replacement mortar mix could be made using: (a) Portland or blended cement, and (b) dolomitic hydrated lime (*a la* ASTM C 207) mixed with (c) natural (canyon) sand, having **1-part Portland (or blended) cement to 1 to 1^1/$_2$-part dolomitic hydrated lime to 4^1/$_2$ to 6-part canyon sand**. Overall appearance of the final mortar would depend on a match on sand that constitutes the dominant proportion of the mortar. Sand to be used should match in color to the color of sand in the present mortar, preferably from the similar source, free of any debris, unsound, clay particles, or any potentially deleterious constituents, should conform to the size requirements of ASTM C 144 for masonry sand, and should be durable. Due to years of atmospheric weathering and alterations, an exact match in color to the existing mortar may not be possible, which, even if possible, could alter in future due to continued atmospheric weathering in the presence of oxygen, moisture, and other elements.

REFERENCES

ASTM C 10, "Standard Specification for Natural Cement," In Annual Book of ASTM Standards, Section Four Construction, Vol. 04.01 Cement; Lime; Gypsum; ASTM Committee C01 on Cement, 2017.

ASTM C 91, "Standard Specification for Masonry Cement," In Annual Book of ASTM Standards, Section Four Construction, Vol. 04.01 Cement; Lime; Gypsum; ASTM Committee C01 on Cement, 2017.

ASTM C 144, "Standard Specification for Aggregate for Masonry Mortar," In Annual Book of ASTM Standards, Section Four Construction, Vol. 04.05 Chemical-Resistant Nonmetallic Materials; Vitrified Clay Pipe; Concrete Pipe; Fiber-Reinforced Cement Products; Mortars or mortars and Grouts; Masonry; Precast Concrete; ASTM Committee C12 on Mortars or mortars for Unit Masonry, 2017.

ASTM C 1324, "Standard Test Method for Examination and Analysis of Hardened Masonry Mortar," In Annual Book of ASTM Standards, Section Four Construction, Vol. 04.05 Chemical-Resistant Nonmetallic Materials; Vitrified Clay Pipe; Concrete Pipe; Fiber-Reinforced Cement Products; Mortars or mortars and Grouts; Masonry; Precast Concrete; ASTM Committee C12 on Mortars or mortars for Unit Masonry, 2017.

ASTM C 270, "Standard Specification for Mortar for Unit Masonry," In Annual Book of ASTM Standards, Section Four Construction, Vol. 04.05 Chemical-Resistant Nonmetallic Materials; Vitrified Clay Pipe; Concrete Pipe; Fiber-Reinforced Cement Products; Mortars or mortars and Grouts; Masonry; Precast Concrete; ASTM Committee C12 on Mortars or mortars and Grouts for Unit Masonry, 2017.

ASTM C 1713, "Standard Specification for Mortars or mortars for the Repair of Historic Masonry," In Annual Book of ASTM Standards, Section Four Construction, Vol. 04.05 Chemical-Resistant Nonmetallic Materials; Vitrified Clay Pipe; Concrete Pipe; Fiber-Reinforced Cement Products; Mortars or mortars and Grouts; Masonry; Precast Concrete; ASTM Committee C12 on Mortars or mortars and Grouts for Unit Masonry, 2017.

ASTM C 51, "Standard Terminology Relating to Lime and Limestone (as used by the Industry)'" In Annual Book of ASTM Standards, Section Four Construction, Vol. 04.01 Cement; Lime; Gypsum; ASTM Committee C07 on Lime, 2017.

ASTM C 856, "Standard Practice for Petrographic Examination of Hardened Concrete," In Annual Book of ASTM Standards, Section Four Construction, Vol. 04.02; ASTM Subcommittee C 9.65, 2017.

ASTM C 1723, "Standard Guide for Examination of Hardened Concrete Using Scanning Electron Microscopy," In Annual Book of ASTM Standards, Section Four Construction, Vol. 04.02; ASTM Subcommittee C 9.65, 2017.

ASTM C 1329, "Standard Specification for Mortar Cement," In Annual Book of ASTM Standards, Section Four Construction, Vol. 04.01; ASTM Subcommittee C01.11, 2016.

ASTM C 150, "Standard Specification for Portland Cement," In Annual Book of ASTM Standards, Section Four Construction, Vol. 04.01; ASTM Subcommittee C01.10, 2018.

ASTM C 1489, "Standard Specification for Lime Putty for Structural Purposes," In Annual Book of ASTM Standards, Section Four Construction, Vol. 04.01; ASTM Subcommittee C07.02, 2015.

ASTM C 207, "Standard Specification for Hydrated Lime for Masonry Purposes," In Annual Book of ASTM Standards, Section Four Construction, Vol. 04.01; ASTM Subcommittee C07.02, 2011.

Bartos, P. Groot, C., and Hughes, J.J. (eds.), "Historic Mortars or mortars: Characteristics and Tests", Proceedings PRO12, RILEM Publications, France, 2000.

Boynton, R., *Chemistry and Technology of Lime and Limestone, 2nd edition*, John Wiley & Sons, Inc. 1980.

Brosnan, Denis, A., Characterization of Rosendale Mortars or mortars For Fort Sumter National Monument and Degradation of Mortars or mortars by Sea Water and Frost Action, Final Report, April 19, 2012.

Callebaut, K., Elsen, J., Van Balen, K., and Viaene, W., "Nineteenth century hydraulic restoration mortars or mortars in the Saint Michael's Church (Leuven, Belgium) Natural hydraulic lime or cement?" Cement and Concrete Research, V 31, pp 397-403, 2001.

Callebaut, K., Elsen, J., Van Balen, K., and Viaene, W., Historical and scientific study of hydraulic mortars or mortars from the 19th century. In International RILEM workshop on historic mortars or mortars: Characterization and Tests; Paisley, Scotland, 12th to 14th May 1999, Edited by Barton, P., Groot, C., and Hughes, J.J., Cachan, France, RILEM Publications, 2000.

Charloa, A.E., "Mortar analysis: A comparison of European procedures." US/ICOMOS Scientific Journal: Historic Mortars or mortars & Acidic Deposition on Stone, 3 (1), pp. 2-5, 2001.

Charola, A.E., and Lazzarin, L., Deterioration of Brick Masonry Caused by Acid Rain, ACS Symposium Series, Vol. 318, pp. 250-258, 2009.

Chiari, G., Torraca, G., and Santarelli, M.L., "Recommendations for Systematic Instrumental Analysis of Ancient Mortars or mortars: The Italian Experience", *Standards for Preservation and Rehabilitation*, ASTM STP 1258, S.J. Kelley, ed., American Society for Testing and Materials, pp. 275-284, 1996.

Doebley, C.E., and Spitzer, D., "Guidelines and Standards for Testing Historic Mortars or mortars", *Standards for Preservation and Rehabilitation*, ASTM STP 1258, S.J. Kelley, ed., American Society for Testing and Materials, pp. 285-293, 1996.

Eckel, Edwin, C., *Cements, Limes, and Plasters*, John Wiley & Sons, Inc. 655pp, 1922.

Edison, M.P. (Editor), *Natural Cement*, ASTM STP 1494, American Society for Testing and Materials, 2008.

Elsen, J., "Microscopy of Historic Mortars or mortars – A Review", *Cement and Concrete Research 36*, 1416-1424, 2006.

Elsen, J., Mertens, G., and Van Balen, K., Raw materials used in ancient mortars or mortars from the Cathedral of Notre-Dame in Tournai (Belgium), Eur. J. Mineral., Vol. 23, pp. 871-882, 2011.

Elsen, J., Van Balen, K., and Mertens, G., Hydraulicity in Historic Lime Mortars or mortars: A Review, In, Valek, J, Hughes, J.J., and Groot, W.P. (Eds.), Historic Mortars or mortars Characterisation, Assessment and Repair, RILEM Book series, Volume 7, pp. 125-139, Springer, 2012.

Erlin, B., and Hime, W.G., "Evaluating Mortar Deterioration", *APT Bulletin*, Vol. 19, No. 4, pp. 8-10+54, 1987.

Goins E.S., "Standard Practice for Determining the Components of Historic Cementitious Materials," National Center for Preservation Technology and Training, Materials Research Series, NCPTT 2004.

Goins, E.S., "A standard method for the characterization of historic cementitious materials." US/ICOMOS Scientific Journal: Historic Mortars or mortars & Acidic Deposition on Stone, # (1), pp. 6-7, 2001.

Groot, C., Ashall, G., and Hughes, J., Characterization of Old Mortars or mortars with Respect to their Repair, State-of-the-art Report of RILEM Technical Committee 167-COM, 2004.

Hughes, D.C., Jaglin, D., Kozlowski, R., Mayr, N., Mucha, D., and Weber, J., "Calcination of Marls to Produce Roman Cement", pp. 84-95, In, Edison, M.P. (Editor), *Natural Cement*, ASTM STP 1494, American Society for Testing and Materials, 2007.

Hughes, J.J., Cuthbert, S., and, Bartos, P., "Alteration Textures in Historic Scottish Lime Mortars or mortars and the Implications for Practical Mortar Analysis", *Proceedings of the 7th Euroseminar on Microscopy Applied to Building Materials*, Delft, pp. 417-426, 1999.

Hughes, R.E., and Bargh, B.L., The weathering of brick: Causes, Assessment and Measurement, A Report of the Joint Agreement between the U.S. Geological Survey and the Illinois State Geological Survey, 1982.

Jana, D., "Application of Petrography In Restoration of Historic Masonry Structures", In: Hughes, J.J., Lesie, A.B. and Walsh, J.A., eds. *Proceedings of 10th Euroseminar on Microscopy Applied to Building Materials*, Paisley, 2005.

Jana, D., "Sample Preparation Techniques in Petrographic Examinations of Construction Materials: A State-of-the-art Review", *Proceedings of the 28th Conference on Cement Microscopy*, International Cement Microcopy Association, Denver, Colorado, pp. 23-70, 2006.

Jedrzejewska, H., Old mortars or mortars in Poland: a new method of investigation, Studies in Conservation 5, pp. 132-138, 1960.

Leslie, A.B., and Hughes, J.J., "Binder Microstructure in Lime Mortars or mortars: Implications for the Interpretation of Analysis Results", *Quarterly Journal of Engineering Geology & Hydrogeology*, V. 35, No. 3, pp. 257-263, 2001.

Lubell, B., van Hees, Rob. P.J., and Groot, Casper J.W.P., The role of sea salts in the occurrence of different damage mechanisms and decay on brick masonry, Construction and Building Materials, Vol. 18, pp. 119-124, 2004.

Martinet, G., Quenee, B., Proposal for a useful methodology for the study of ancient mortars or mortars, Proceedings of the International RILEM workshop "Historic Mortars or mortars: Characteristics and tests," Paisley, pp. 81-91, 2000.

Mack, Robert, and Speweik, John P., *Preservation Briefs 2*, U.S. Department of the Interior, National Park Service Cultural Resources, Heritage Preservation Services, pp. 1-16, 1998.

Middendorf, B., Baronio, G., Callebaut, K, and Hughes, J.J., "Chemical-mineralogical and physical-mechanical investigation of old mortars or mortars, Proceedings of the International RILEM workshop "Historic Mortars or mortars: Characteristics and tests," Paisley, pp. 53-61, 2000.

Middendorf, B., Hughes, J.J., Callebaut, K., Baronio, G., and Papayanni, I., Mineralogical characterization of historic mortars or mortars, In. Groot, C., et al. (eds), Characterisation of Old Mortars or mortars with Respect to their Repair, State-of-the-art Report of RILEM Technical Committee 167-COM, pp. 21-36, 2004a.

Middendorf, B., Hughes, J.J., Callebaut, K., Baronio, G., and Papayanni, I., Chemical characterization of historic mortars or mortars, In. Groot, C., et al. (eds), Characterisation of Old Mortars or mortars with Respect to their Repair, State-of-the-art Report of RILEM Technical Committee 167-COM, pp. 37-53, 2004b.

Middendorf, B., Hughes, J.J., Callebaut, K., Baronio, G., and Papayanni, I., "Investigative Methods for the Characterization of Historic Mortars or mortars – Part 1: Mineralogical Characterization," *Materials and Structures*, Vol. 38, 2005a.

Middendorf, B., Hughes, J.J., Callebaut, K., Baronio, G., and Papayanni, I., "Investigative Methods for the Characterization of Historic Mortars or mortars – Part 2: Chemical Characterization," *Materials and Structures*, Vol. 38, pp 771-780, 2005b.

Sarkar, S.L., Aimin, Xu, and Jana, Dipayan, Scanning electron microscopy and X-ray microanalysis of Concretes, pp. 231-274, In, Ramachandran, V.S. and Beaudoin, J.J. Handbook of Analytical Techniques in Concrete Science and Technology, Noyes Publications, Park Ridge, New Jersey, 2000.

Speweik, J.P., *The History of Masonry Mortar in America 1720-1995*, 2010.

Stewart, J., and Moore, J., Chemical techniques of historic mortar analysis, Proceedings of the ICCROM Symposium "Mortars or mortars, Cements, and Grouts used in the Conservation of Historic Buildings," Rome, ICCROM, Rome, pp. 297-310, 1981.

Valek, J., Hughes, J.J., and Groot, C. (eds.), *Historic Mortars or mortars: Characterization, Assessment and Repair*, Springer, RILEM Book series Vol. 7, p. 464, 2012.

Valek, J., Hughes, J.J., and Groot, C. (eds.), Historic Mortars or mortars: Characterization, Assessment and Repair, Springer, RILEM Book series Vol. 7, 2012.

Van Balen, K., Toumbakari, E.E., Blanco, M.T., Aguilera, J., Puertas, F., Sabbioni, C., Zappia, G., Riontino, C., and Gobbi, G., "Procedures for mortar type identification: A proposal." In International RILEM workshop on historic mortars or mortars: Characteristics and Tests; Paisley, Scotland, 13th to 14th May 1999, edited by Barton, P., Groot, C., and Hughes, J.J., Cachan, France: RILEM Publications, 2000.

Vyskocilova, R., W. Schwarz, D. Mucha, D. Hughes, R. Kozlowski, and J. Weber, "Hydration processes in pastes of roman and American natural cements," *ASTM STP*, vol. 4, no. 2, 2007.

Weber, J., Gadermayr, N., Kozlowski, R., Mucha, D., Hughes, D., Jaglin, D., and Schwarz, W., Microstructure and mineral composition of Roman cements produced at defined calcination conditions, Materials Characterization, Vol. 58, pp. 1217-1228, 2007.

✪ ✪ ✪ END OF TEXT ✪ ✪ ✪

END OF REPORT[2]

[2] The CMC logo is made using a lapped polished section of a 1930's concrete from an underground tunnel in the U.S. Capitol.